AN INVESTIGATION

OF

ISOLATED BURSTS

OF SOLAR RADIO NOISE.

A thesis presented for the degree of
Master of Science of Rhodes University,

by

W. L. H. SHUTER. B.Sc (Hons.) Rhodes.

Department of Physics,
Rhodes University,
GRAHAMSTOWN.
South Africa.

September, 1958.

CONTENTS

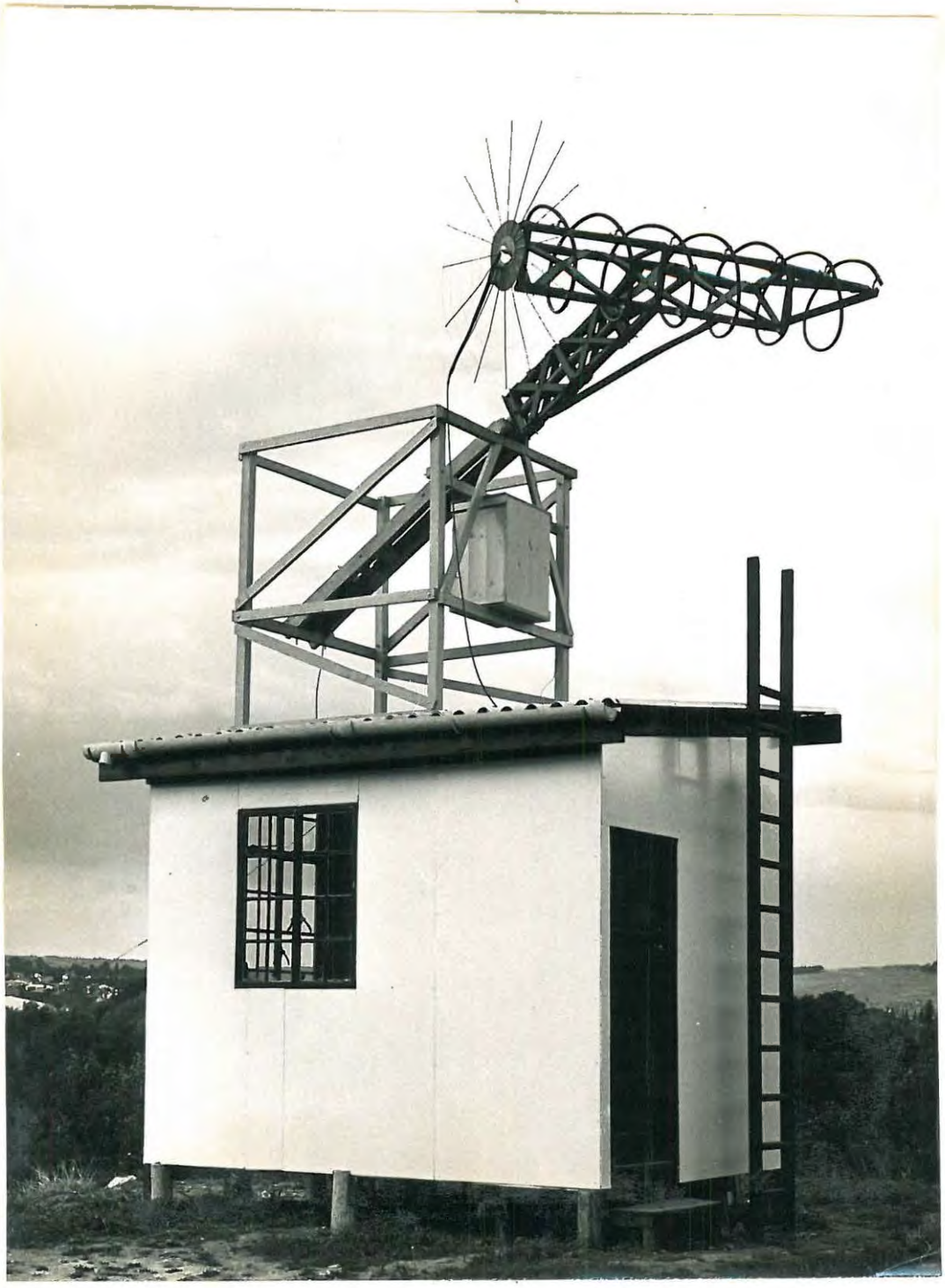

PLATE A. The Rhodes University solar radio telescope.

PLATE B. The Helical Antenna.

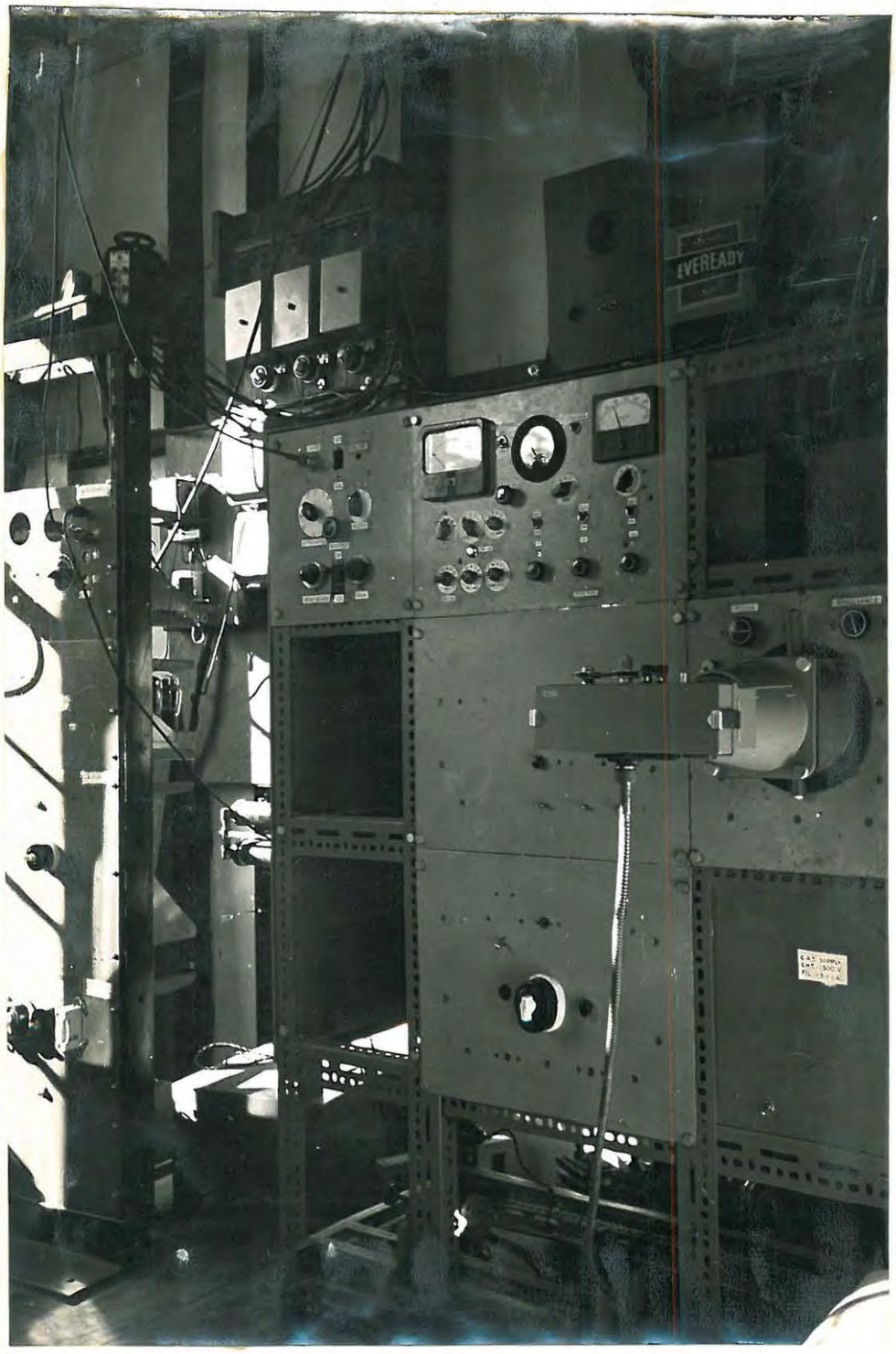

PLATE C. The interior of the shack.

HISTORY OF THE PROJECT

The aim of this research project, to take place during the I.G.Y., was to determine the dynamic spectra of bursts of solar radio frequency noise in the frequency band 100-500 Mc./s. and to investigate:-

(1) The degree of correlation between bursts, and visual solar phenomena, such as flares, sunspots, prominences etc.

(2) The incidence of harmonics in solar bursts, and comparison of the paths of exciting agencies in the solar atmosphere, as deduced from the dynamic spectra, with the observed positions and movements of flares.

This involved the construction of a swept frequency radio noise receiver covering the above mentioned frequency range in three channels.

Channel 1 :- 100-200 Mc./s.

Channel 2 :- 200-350 Mc./s.

Channel 3 :- 350-500 Mc./s.

Each channel was to consist of a broad band helical antenna, a swept frequency pre-amplifier comprising Cascode R.F. amplifier, first detector and first I.F. amplifier, housed in a box on the antenna mast. Signals from this were to be fed via co-axial cable to three main I.F. amplifiers situated in the receiver hut.

The outputs of the three second detector stages in the I.F. amplifiers were to be applied to a gain-equalizer and channel-mixer. The function of the gain-equalizer was to compensate for differences in receiver gain at different frequencies in such a manner that the resulting gain over the entire frequency range was constant.

The output of this stage was to feed two D.C. amplifiers, and thence two cathode ray tubes, one of which was to have the usual "A" type scan, and the other was to be intensity modulated.

Dr. E.F. Stack-Forsyth began to construct the power supplies for the equipment in the latter half of 1956. In January 1957 he was joined in this project by Mr. J.O. Speedy (C.S.I.R. technical assistant) and the author, and work on channel 1 commenced immediately.

A site was eventually found for the equipment next to the Rhodes University men's hockey field, and the geographical co-ordinates of a beacon placed there were determined by a Government surveyor.

A "shack" to house the equipment was built by J.O. Speedy and the author - see plate A - and was completed by the middle of May. The helical antenna, which had been constructed and tested by the author, was mounted equatorially on the mast above the roof - see plate B -.

Shortly afterwards a power line was laid on by the municipality, and a private telephone line connecting the Physics department to the shack was installed. The telephone line was used to transfer half minute pulses from a Synchronome clock in the Physics department to a master relay in the shack which controlled a slave clock, the antenna drive, and produced time marks on the records.

Meanwhile, Dr. Stack-Forsyth had been experiencing a lot of difficulty in the construction of the swept frequency pre-amplifier, and being without proper test equipment at the time progress was necessarily slow.

During July he decided, as an interim measure, to construct a fixed frequency pre-amplifier (tuned to 120 Mc./s.) in order to obtain results as soon as possible, and on August 9 1957, the first record was obtained by photographing the output from the second detector as it appeared on the screen of a Cossor double beam oscilloscope. During August and September a cathode ray oscilloscope display unit and a D.C. amplifier were constructed.

At the end of September Mr. J.O. Speedy left the project and Mr. R.G. Speedy took his place.

By October the equipment was in more or less regular operation. On October 23 there was a partial eclipse of the sun over Grahamstown from sunrise (03:24 U.T.) until (04:32 U.T.) and the equipment was run between the hours of (03:00 U.T.) and (05:00 U.T.) on the day of the eclipse, and also on October 22 and October 24 as control days. However, as the receiver was not capable of

..

detecting the thermal component of solar radio noise, and as there were no outbursts during the time of observation, no eclipse effects were noticed.

In November the pre-amplifier showed instability on 120 Mc./s. and was retuned to 125 Mc./s. This thesis is based on observations of solar radio noise on 125 Mc./s. taken during the period November 26 1957 — February 6 1958. After February 6 the apparatus was run at a lower gain setting in order that outbursts might be observed, and the records obtained are not suitable for analysis of isolated bursts.

The only data on visual solar phenomena available to the author for the above mentioned period was the "Daily Maps of the Sun" issued by the Fraunhofer Institute. These maps give the position, and sometimes the duration, of solar flares but they do not give the time of maximum of flares or any other details. They proved to be quite inadequate for any investigation of the degree of correlation existing between solar radio noise outbursts and solar flares.

In view of this, the author has decided to investigate isolated bursts of solar radio noise, which at the time (February 1958) were thought to show no correlation with visual phenomena on the sun.

Shortly after this decision had been made, the author discovered that Loughhead, Roberts, and McCabe (1957) had established that there is a high degree of association of isolated bursts with microflares. In spite of this, the investigation was continued and the results of it are presented in the pages following.

ACKNOWLEDGEMENTS

The author wishes to express his sincere appreciation and thanks to:

Dr. E. F. Stack-Forsyth for supervision of this research, and for the active interest he has shown in it;

Professor J. A. Gledhill for his encouragement in all phases of this research;

The South African Council for Scientific and Industrial Research for a research grant and a research bursary;

Messrs J. C. Speedy and R. G. Speedy for their co-operation in all matters connected with this research;

Mr. A. R. Scanlon for assistance with the construction of apparatus used;

Mr. G. F. Walters for photographic plates A, B, and C appearing in this thesis.

NOTE ON THE DIVISION OF LABOUR

Below is listed the contribution of each member to the joint research project during 1957 :

Dr. E. F. Stack-Forsyth: General supervision of policy and design. The design, construction and testing of the H.T. and L.T. power supplies, the fixed frequency pre-amplifier, the I.F. amplifiers, the channel-mixer and gain-equalizer.

W. L. H. Shuter: The design, construction and testing of a broad band helical antenna operating in the frequency range 110 - 190 Mc./s. ; design and construction of the antenna drive; construction of a cathode ray tube output indicator and associated E.H.T. supply; construction of an audio amplifier for aural monitoring of received signals; part construction of the shack.

J. C. Speedy: The construction of electronic voltage regulators for the pre-amplifier, the I.F. amplifiers, and the D.C. amplifier; construction of the D.C. amplifier; construction of the camera drive; part construction of the shack.

R. G. Speedy: The running and maintenance of the equipment; construction of a monitor panel to facilitate fault tracing, and operation of the equipment.

ABSTRACT

The literature on isolated bursts and possible mechanisms of origin has been critically reviewed, and observations point to a mechanism involving emission of electromagnetic radiation from plasma oscillations in the solar corona excited by outward travelling disturbances. Solar noise observations on 125 Mc./s. recorded at Rhodes University during the period November 26 1957 - February 6 1958 have been analysed by the author for isolated bursts, and these observations show the same general features reported by previous investigators. In interpretation of these records particular attention has been devoted to two aspects of isolated bursts; namely, the preponderance on single frequency records of double-humped bursts, and the shapes of isolated burst profiles. The author suggests that a probable explanation of double-humped bursts observed on any frequency f is that the first hump represents emission at or near the level of zero refractive index for f radiation, and that the second hump corresponds to harmonic emission at the f/2 level. Source velocities may be calculated from the time delay between the peaks, and an average value of 2×10^4 km./sec. was obtained from an analysis of 21 double-humped bursts. This value is in very good agreement with that deduced by Wild (1950b) from the rate of frequency drift of peak intensity of isolated bursts. Simple isolated bursts have decay profiles which are approximately exponential in shape, and this is usually interpreted in terms of the natural decay of plasma oscillations in the medium of origin. The author has verified that the exponential function is a good fit to the observed decay profiles, but shows that a relation of the form $I^{-1/n} \propto t$ (where I is intensity and t is time) fits just as well. An alternative model is suggested which would lead to an exponential-like decay profile which is not determined by the natural decay of plasma oscillations. The work concludes with some suggestions for further research.

CHAPTER ONE

THE EQUIPMENT

The equipment comprises the Rhodes University solar radio noise receiver, operating on a frequency of 125 Mc./s.,

Geographical co-ordinates: Latitude: South 33° 18' 38.85"

Longitude: East 26° 31' 07.73"

situated in Grahamstown, C.P., South Africa.

A radio telescope consists essentially of an antenna system, a radio receiver, and a recording device. A block diagram of the Rhodes University radio noise receiver is shown below:

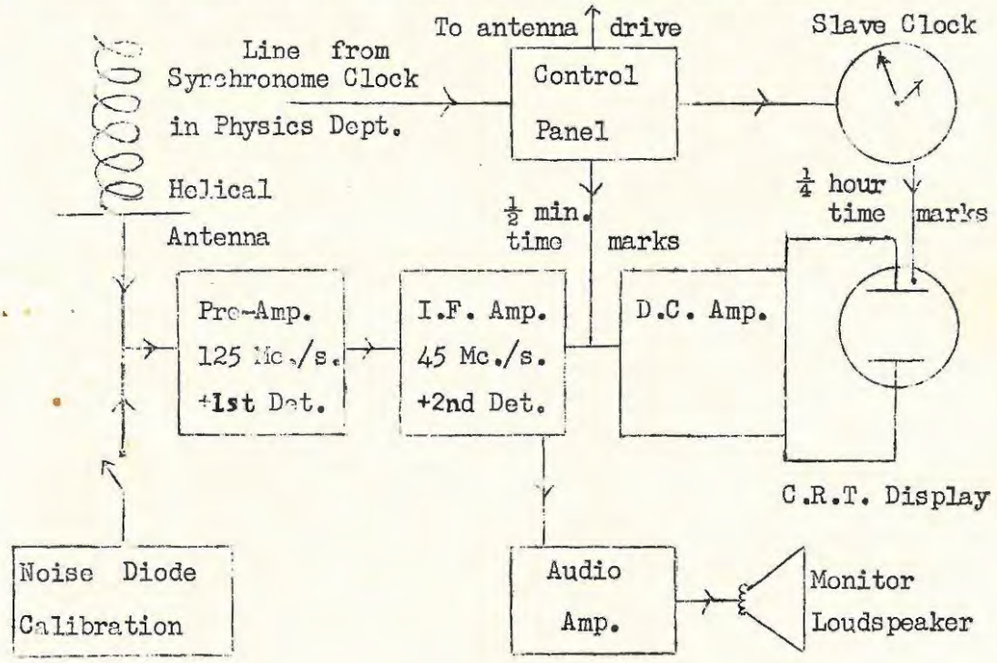

The above receiver works on the conventional superheterodyne principle. A 125 Mc./s. signal, received by the antenna, is amplified in the pre-amplifier and converted to the intermediate frequency of 45 Mc./s. This is amplified in the main I.F. amplifier and detected. The resulting fluctuating D.C. voltage is amplified in a D.C. amplifier, and applied to the Y-plates of a cathode ray oscilloscope, causing the spot on the cathode ray tube to move up and down. This spot is photographed on film moving in the X-direction, and hence a continuous trace of intensity versus time is obtained.

2/.....

(a) The Helical Antenna:-

The basic requirements for the antenna at the time of construction were:

(1) The ability to receive radiation along the principal axis of the antenna, over a broad band of frequencies, with little variation of gain.

(2) A minimum of side lobes in the polar diagrams of the antenna, in order that the amount of local interference received by the antenna be a minimum.

Two types of antenna meet the above specifications - the rhombic antenna, and the helical antenna operating in the so-called beam or axial mode. The helical antenna was chosen because its polar diagrams in general show less side lobes than those of the rhombic antenna, and also because it is a more compact type of antenna and is thus easier to mount.

Characteristics of helical antennas operating in the axial mode:-

A helix with a diameter of about one wavelength can receive radiation along its axis. Radiation is a maximum in the direction of the axis, and only one circularly polarized component of the received radiation is accepted. In the case of a right-handed helix, right-handed circularly polarized radiation is accepted completely, left-handed circularly polarized radiation is rejected, and only the right-handed circularly polarized component of plane polarized radiation is accepted.

For the axial mode, the phase velocity of wave propagation along the helix is such as to make the component electric fields from each turn of the helix add nearly in phase, along the direction of the helix axis. The tendency for this to occur is so strong that the phase velocity adjusts itself to produce this result. This natural adjustment of the phase velocity is one of the most important characteristics of wave transmission in the helix. It is this fact

which accounts/...

THE HELIX

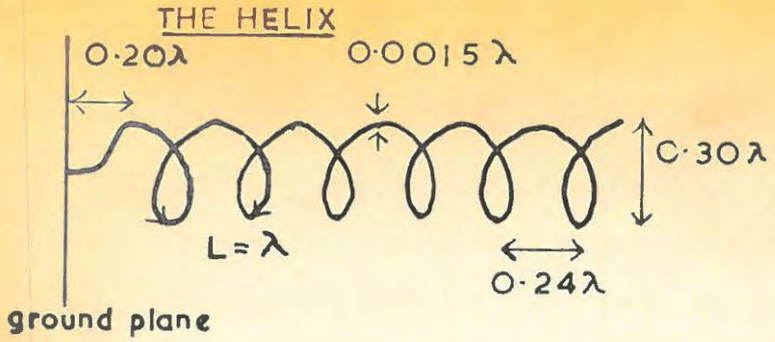

$\lambda = 200\,cm.$

THE GROUND PLANE

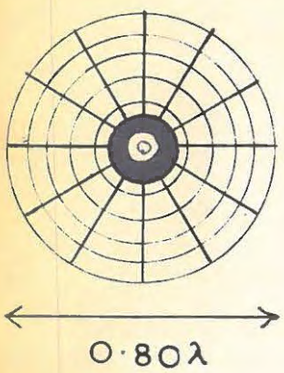

THE MATCHING TRANSFORMER

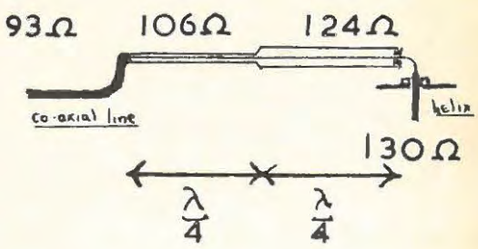

POLAR DIAGRAMS FOR HELICAL ANTENNA

arbitrary power scale: linear

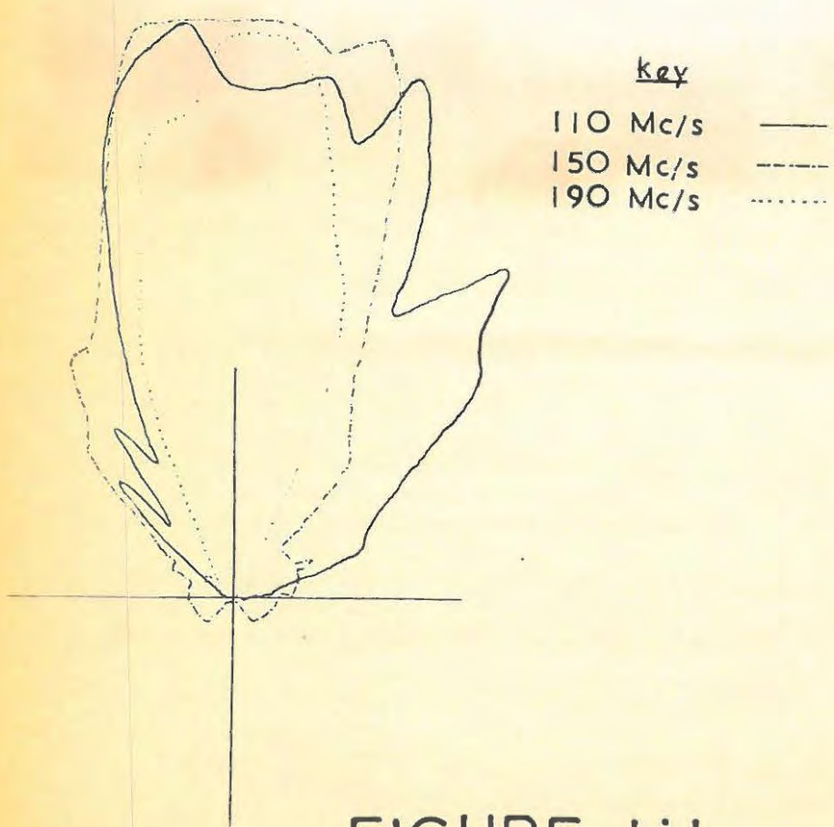

FIGURE 1:1

which accounts for the persistence of axial mode radiation patterns over such a wide frequency range.

Design, construction and testing of the helical antenna:-

The helix constructed is the "optimum helix" described by Kraus (1948). It is optimum in the sense that it has the most uniform radiation and impedance characteristics over the greatest frequency range. The helix was designed to have a central frequency of 150 Mc./s., in order to cover the frequency band 110-190 Mc./s. Its dimensions are shown in figure 1:1.

A helix, of six turns wound in a right-handed sense, with a pitch angle of 14°, was constructed. It was backed by a ground plane- see figure 1:1 -which is described by Kraus (1948). No facilities were available at the time for measuring the terminal impedance of the antenna, so Kraus's value of 130 ohms was assumed. A broad band matching transformer consisting of two quarter-wave co-axial sections with impedances of 124 ohms and 106 ohms respectively- see figure 1:1 -was designed and constructed along lines suggested by Slater (1942), to convert the antenna terminal impedance to that of the 93 ohm co-axial line leading to the input of the pre-amplifier.

Polar diagrams in one plane were plotted for the antenna at frequencies of 110,150 and 190 Mc./s. The experimental procedure for obtaining the polar diagrams was as follows:

A low powered transmitter, operating in the frequency range 100-200 Mc./s. and feeding a vertical folded dipole antenna, was placed in the centre of a hockey field, in order to be far away from obstacles that could cause undesirable reflections. The transmitter was tuned to the desired frequency, and thereafter its gain was not altered. The receiving helix, situated at a height of about three feet above the ground, was placed about eight wavelengths away, so that the received wave front was effectively plane, and was rotated in 5° steps, the relative power received at the antenna terminals being read on a simple field strength meter.

By assuming/....

By assuming that the lobe shape of the antenna in three dimensions was of the form that would be obtained by rotating the observed polar diagram about its principal axis- a justifiable assumption in view of the fact that the polar diagrams for E_θ and E_ϕ given by Kraus (1948) are very nearly coincident -the directive gain, or directivity "g" of the antenna at any particular frequency may be calculated from the polar diagrams.

For receiving antennas the directive gain "g" may be defined as the ratio of the power absorbed in a load matched to the antenna from a given signal arriving in the direction of maximum gain, to the power absorbed from the same signal averaged over all antenna orientations.

The directive gain may also be expressed in terms of the equivalent number of decibels:

$G = 10 \log_{10} g$ decibels.

It is a general property of antennas that the directivity is related to the effective receiving area "A" of the antenna by the well known relation:

$$g = \frac{4\pi A}{\lambda^2}$$

The quantities g,G,A, and the beamwidth to half power points, were evaluated from the polar diagrams for the antenna at frequencies of 110,150, and 190 Mc./s., and are tabulated below:

f Mc./s.	110	150	190
g	18.3	32.2	87.8
G db.	12.6	15.1	19.4
A sq.met.	10.8	10.2	17.4
Beamwidth	80°	60°	40°

The whole assembly, consisting of the helix mounted on ceramic insulators attached to a triangular wooden framework, the ground plane, and the matching transformer, was then mounted equatorially, the declination being adjustable in order to track the sun throughout the year.

(b)/...

(b) The Antenna Drive:-

Requirements for the antenna drive were:

(1) Simplicity of construction.

(2) Simplicity and reliability of operation.

(3) That it be independent of frequency and voltage fluctuations of the A.C. mains.

The antenna drive designed and constructed by the author met all the above specifications admirably. It is a modified form of a drive designed by Gerrish in 1900 for use with optical telescopes, and is illustrated in figure 1:1A.

The drive is powered by an A.C. motor F, which has a crank G attached to its drive shaft. The rotary motion of this crank is converted to reciprocatory motion of a rod I by means of a connecting rod and a piston rod. Rod I has a tooth J at its end which is held in contact with a ratchet wheel K, having 19 teeth, by means of a spring. One rotation of the crank causes the tooth J to pull at one tooth of the ratchet wheel and get back into position to pull at the next tooth. A spring loaded pawl L prevents the ratchet from rotating in the opposite direction. The ratchet is connected to a 150:1 reduction gear, which turns the helical antenna about the polar axis of the equatorial mount.

The motor is actuated by half minute impulses from a Synchronome clock in the Physics department, and each impulse causes crank G to perform one revolution, and then to switch the motor off. This process takes less than one second. Thus, just after each half minute impulse, the ratchet wheel is turned through 360/19 degrees of arc. This motion is applied to the polar axis drive shaft via a reduction gear with a 150:1 ratio. The polar axis shaft thus moves through 360/ (19 x 150) = 0.126 degrees per half minute, or 15.1 degrees per hour. The error in tracking the sun is about 0.1 degrees per hour, which is negligible in view of the large beamwidth of the helical antenna. This drive only works in one direction, and to reset the antenna at the end of a day's run, the pawl is disengaged and the ratchet is turned in the opposite direction manually.

The action/ .....

The action of the switching mechanism for the drive motor is as follows:

Every half minute the points of relay A, situated in the Physics department, are momentarily closed by a relay on the Synchronome clock. This produces an impulse which is carried along a telephone line to the shack, and causes the points of relay B, the shack master relay, to close momentarily. During this period the relay C is energized and its points close. An alternate circuit going through points E, which are normally closed, holds relay C closed and thus prevents points C from opening when points B open. In addition relay C operates a mercury switch D, which closes when the relay is energized. Closing of the mercury switch D actuates motor F which begins to rotate. After it has turned crank G through one revolution, a projection H on crank G momentarily opens points E, and the circuit for relay C is broken. The mercury switch opens, and switches off the motor.

From the above description it can be seen that the rate of drive is governed only by:

(1) The frequency of impulses from the Synchronome clock.

(2) The number of teeth on the ratchet wheel.

(3) The gear ratio of the reduction gear between the ratchet wheel and the polar axis drive shaft.

Frequency and voltage fluctuations of the A.C. mains do not affect the rate of drive, since this is independent of the speed of the drive motor. However the drive can only work if the time of revolution of crank G is smaller than the time between actuating impulses.

The drive proved extremely simple and inexpensive to construct. The motor used was a fractional horse power motor from a washing machine, which turned the crank through a built-in reduction gear. The ratchet wheel, connecting rod, and piston, were constructed in the Rhodes University workshops, and the reduction gear to the polar axis drive shaft came from an Avro-Anson landing gear. The relay and mercury switch C,D, was ex-army stock.

This drive"....

PRE-AMPLIFIER CIRCUIT DIAGRAM

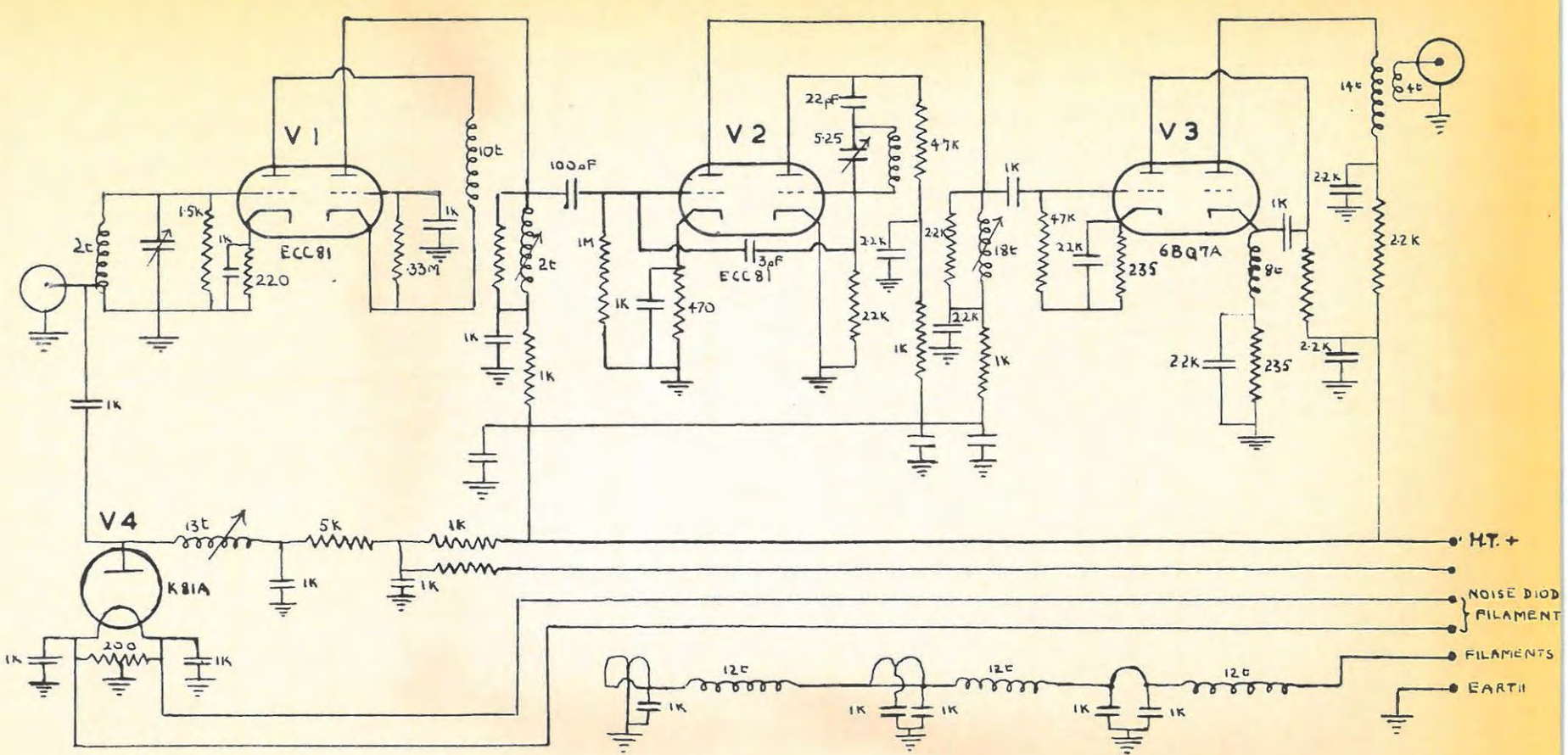

FIGURE 1:2

This drive has proved to be extremely reliable in operation, the only maintenance required being occasional lubrication of the moving parts and cleaning of the relay points. The author believes that a drive of this nature would be highly suitable for antenna systems to be constructed in the future at Rhodes University.

Setting of the antenna to compensate for changes in the sun's declination throughout the year is done manually. Provision is made for changing the angle the helix axis makes with the declination axis of the equatorial mount in steps of 7 degrees. The error introduced by having such large steps is negligible in view of the fact that the beamwidth of the antenna at 125 Mc./s. is about 70°. The dates upon which these adjustments must be made, are obtained from tables of the sun's daily declination in the Nautical Almanac.

(c) The Pre-Amplifier:-

The circuit diagram of the fixed frequency (125 Mc./s.) pre-amplifier is shown in figure 1:2.

It consists of a Cascode R.F. amplifier V1, mixer and local oscillator V2, and a Cascode I.F. amplifier V3. The "noise" diode V4 is permanently connected across the input, and is brought into operation by applying filament heating power.

The principal parameters of the pre-amplifier are quoted below:

Centre frequency:	125 Mc/s.
Bandwidth:	1.75 Mc/s.
Gain, from input to output:	24 db.
Noise figure:	7.8 db.

(d) The I.F. Amplifier:-

This consists of a modified Pye 45 Mc./s. I.F. strip. The final cathode follower of the Pye strip is used to drive a monitor loudspeaker via an amplifier.

Centre frequency:	45 Mc./s.
Gain:	74-86 db.
Bandwidth:	2.4-1.7 Mc./s.

(e)/...

(e) The D.C. Amplifier:-

An input attenuator is used to reduce the signal from the negative side of the second detector output in the I.F. strip. To permit more sensitive signal observation, a positive buck-out voltage is used to balance out the background noise output from the detector. Ganged with the range switch for the signal attenuator is the buck-out voltage attenuator. This has the same ratios as the signal attenuator, so that alteration of the latter should not affect the proportion of the signal bucked-out.

After attenuation and buck-out, the signal is fed to the D.C. amplifier through an RC filter with a time constant of one millisecond. The purpose of this is to smooth out rapid fluctuations of the input signal, so that photography of the C.R.T. spot is possible.

The D.C. amplifier is a two-stage difference amplifier, with a cathode follower output. It is operated so that with zero input signal, the amplifier is unbalanced in one direction. Signals of increasing magnitude bring it into balance, and then out of balance in the opposite direction.

The advantages of this are two-fold:

(1) The full height of the C.R.T. screen is used.

(2) The range of operation of the amplifier is doubled.

A relay placed across the input to the amplifier is energized by pulses from the Synchronome clock at half minute intervals. This short circuits the input and thus provides a time mark, and also establishes the base level of the record. It also has the effect of shorting out nearly all of the interference produced by the switching system of the antenna drive.

(f) The Display:-

The output from the D.C. amplifier is applied to the Y-plates of a Dumont 5ADP cathode ray tube, with a blue-fluorescent screen. The X-plates are connected together, and joined to the accelerator, so that no deflection of the spot is produced in the X-direction.

The spo / ....

The spot is photographed on Eastman Positive 35 mm. film, moving in the X-direction at the rate of 1.6 cms. per minute.

Pulses are obtained from the slave clock every fifteen minutes, and these cause a small bulb, situated next to the C.R.T. screen in the same vertical line as the spot, to flash, thus providing quarter hourly time marks on the records.

(g) Power Supplies and Electronic Voltage Regulators:-

The H.T. rectifier is of the conventional type. The L.T. rectifier comprises a bridge circuit of selenium rectifiers. All supply voltages are electronically regulated, with the exception of the cathode ray tube E.H.T. supply. The regulators are conventional circuits consisting of:

(1) Series control tubes.

(2) A D.C. amplifier consisting of a difference amplifier working into a pentode.

(h) Calibration:-

A noise diode, mounted on the pre-amplifier chassis, and connected in parallel with the antenna, is used for intensity calibration of the receiver.

The mean-square value of the noise current, i_n^2, from a temperature limited diode, in the frequency band B, is:

$$i_n^2 = 2 e I B$$

where I is the mean current passing between the anode and cathode of the diode, and e is the electronic charge (1.59×10^{-19} coulombs).

The available power at the receiver input is therefore:

$$P(\text{diode input}) = \tfrac{1}{2} (i_n^2) \times \tfrac{1}{2}Z \qquad (1.1)$$

$$= \tfrac{1}{2} e I B Z \qquad (1.2)$$

where Z is the input impedance of the receiver. The factor $\frac{1}{2}Z$ in (1.1) arises from the fact that the impedance of the antenna is in parallel with the input impedance of the receiver, and these

impedances/.....

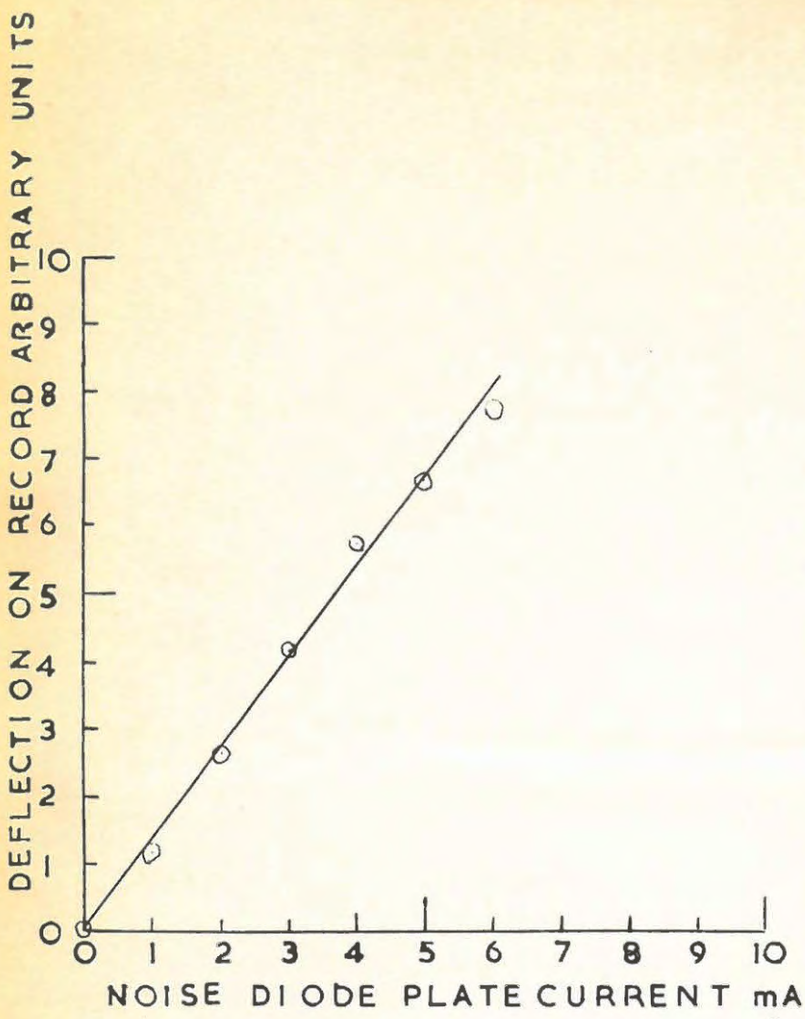
DEFLECTION ON RECORD ARBITRARY UNITS
0
1
2
3
4
5
6
7
8
9
10
0 1 2 3 4 5 6 7 8 9 10
NOISE DIODE PLATE CURRENT mA

FIGURE 1:3

impedances are equal when matched for optimum power transfer from the antenna to the receiver.

The power received by an antenna, if D is the flux density of an incoming signal, and A is the effective receiving area of the antenna, is:

$$P_{(antenna)} = D\ A\ B$$

Therefore the available power at the receiver input is:

$$P_{(antenna\ input)} = \tfrac{1}{2}\ D\ A\ B \qquad (1.3)$$

When the received power is equal to the power produced by the noise diode, from (1.2) and (1.3):

$$\tfrac{1}{2}\ D\ A\ B = \tfrac{1}{2}\ e\ I\ B\ Z$$

$$\therefore\ D = \frac{e\ I\ Z}{A} \qquad (1.4)$$

Substituting numerical values in (1.4) - Z = 125 ohms, A = 10.8 square metres at 125 Mc./s.- the following relation is obtained:

$$D = 1.85 \times 10^{-21}\ I'\ \text{watts/metres}^{+2}/(\text{c./s.}) \qquad (1.5)$$

where I' is the noise diode plate current in milliamps.

This relation is used to calculate the intensities of bursts and outbursts of solar radio noise recorded by the equipment.

The calibration process involves increasing the plate current of the noise diode in steps from 0-10 milliamps, by increasing the noise diode filament current. Calibration is performed with the antenna connected, so it is done during "quiet" periods of the day.

A typical graph of deflection produced on the records (in arbitrary units) versus noise diode plate current - proportional to the flux density of incoming signals from (1.5) - is shown in figure 1:3.

This graph is in effect a representation of the receiver gain law, and it may be seen from the graph that the overall gain of the receiver is linear.

(i) Transient Response/...

(i) Transient Response:-

Two main factors determine the response of the equiment to transients.

(1) The time constant of the filter circuit in the D.C. amplifier, which is of the order of one millisecond.

(2) The slow film speed (1.6 cms. per minute) which has the effect of blurring very rapid fluctuations of the signal.

Isolated bursts, considered in this thesis, have smooth profiles, and their time of rise and fall, which is of the order of seconds, is large compared with the time constant of the output circuit. Thus, bearing in mind that the overall gain of the receiver is linear, the profiles of isolated bursts, as observed on the records, may be taken to be a faithful representation of the radiation incident upon the antenna.

BIBLIOGRAPHY.

PAWSEY, J.L., BRACEWELL,R.N. 1955 Radio Astronomy, Ch.II, (Clarendon:Oxford)
A good account is given of the instrumental techniques used in the observation of extraterrestial radio noise.

SCHELKUNOFF,S.A., FRIIS,H.T. 1952 Antennas, (Chapman and Hall:London)
This is a comprehensive book on antenna design.

The properties of helical antennas are described in detail in the following references:

KRAUS,J.D. 1947 Electronics, 20, 109.

KRAUS,J.D. 1947 Proc.Inst.Radio Engrs., 35, 265.

KRAUS,J.D. 1948 Proc.Inst.Radio Engrs., 36, 1236.

KRAUS,J.D., WILLIAMSON,J.C. 1948 J.appl.Phys., 19, 87.

GLASSER,O.J., KRAUS,J.D. 1948 J.appl.Phys., 19, 193.

JONES,G.C. 1956 Proc.Instn.Elect.Engrs., B 103, 764.

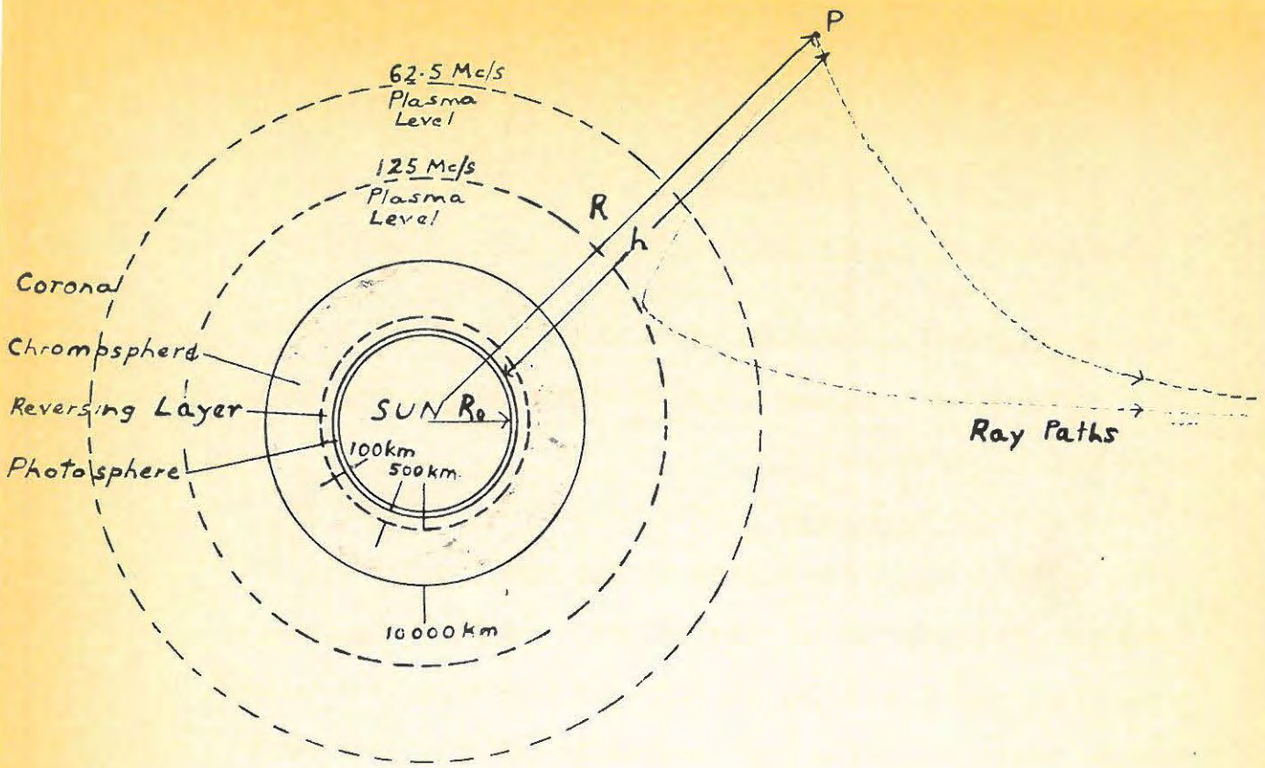

The Solar Atmosphere

(Not to scale)

FIGURE 2:1

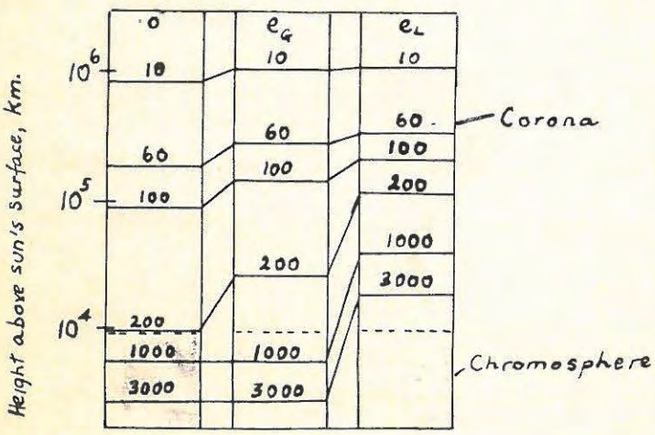

Levels of zero refractive index in the solar atmosphere at different radio frequencies. The levels are shown at 30° latitudes; O refers to the ordinary ray, e_G and e_L refer to the extra-ordinary ray for the general magnetic field and for the region above a large sunspot (H_0 = 3 600 oersteds) respectively. The numbers on the lines give the wave frequency in Mc/s.

Smerd (1950)

FIGURE 2:2

CHAPTER TWO

SOME ASPECTS OF SOLAR PHYSICS RELEVANT TO RADIO ASTRONOMY.

A: A QUALITATIVE DESCRIPTION OF THE SOLAR ATMOSPHERE.

The solar atmosphere consists of four main layers, which are depicted in figure 2:1.

(1) The Photosphere

This layer, which is only 100 km. thick, is the visible surface of the sun. It is known to emit a continuous spectrum in the ultra-violet, visible, and infra-red regions, with a maximum of intensity at 4 740 $\mathring{A}$. The energy distribution of this continuous spectrum agrees approximately with that for a black body at 6 000^{o} K.

(2) The Reversing Layer

This layer extends for several hundred km. above the photosphere, and is simply a layer of transition between the photosphere and the chromosphere.

(3) The Chromosphere

The chromosphere extends from about 500 - 15 000 km. above the photosphere, and shows bright emission lines of both neutral and ionized atoms. The temperature of the lower chromosphere is approximately 3×10^{4} ^{o}K.

(4) The Corona

This is situated above the chromosphere and extends for several million km. The light of the corona consists mainly of photospheric light scattered by fast moving free electrons. In addition there are a number of bright emission lines due to highly ionized atoms (eg. iron atoms which have lost up to 14 electrons). In order to explain this high degree of ionization, and the great width of the coronal emission lines caused by the Doppler effect, it is necessary to postulate a kinetic electron temperature of the order of 1×10^{6} ^{o}K. The electron temperature decreases in the outer regions of the corona, and seems to fall below

1×10^{6} ^{o}K/.....

1×10^6 °K for heights greater than 10^5 km. above the photosphere. Localized bright patches have been observed in the corona where the temperature appears to be several million degrees. The intensity of light emitted by the outer layers of the solar atmosphere is very much less than the intensity of photospheric light, and hence optical observations of the outer layers are only possible during eclipse conditions, or with artificial blacking out of the sun's disk. Because of the inherent difficulties of observation, the data which result are not known with precision.

B: SOME FEATURES OF THE DISTURBED SUN

Disturbances on the sun appear to occur in so-called "centres of activity". Among such disturbances the most prominent are sunspots, solar flares and prominences.

(1) Sunspots

Viewed through a telescope sunspots appear as a dark central core (the umbra) surrounded by less dark filaments (the penumbra) situated on the photosphere. They are irregular in shape, and range in size from huge areas of diameter about one geocentric minute of arc or 50 000 km. to the limit of resolution of viewing instruments. All sunspots have strong magnetic fields, and the field strength decreases from values of up to 4 000 oersteds at the centre of the spot to very small values not far outside the penumbra. Sunspots tend to occur in groups, and members of a sunspot group show both magnetic polarities. The flux from the leading spot returns largely through the remaining members, although there is usually an excess which returns through the unspotted photosphere.

Individual spots appear in an unpredictable manner, but statistically their incidence is governed by the well known 11 year cycle. They tend to appear only on two restricted zones of the sun's surface. These zones, which are about 15° wide, fluctuate in latitude with the sunspot cycle. At the beginning of an 11 year cycle they are centred on latitudes of $\pm 28^\circ$, and they

move towards/.....

move towards the solar equator, reaching latitudes of $\pm 10^{\circ}$ at the end of the cycle.

Ryle and Vonberg (1948), using a spaced aerial interferometer, established the fact that circularly polarized radio waves are emitted from regions on the sun which are not greater than 10 minutes of arc, and came to the important conclusion that these circularly polarized radio waves are emitted from regions which are of the same order of size as visual sunspots.

(2) Chromospheric Eruptions or Solar Flares

A solar flare may be described as a small area in the disturbed environment of a sunspot which emits the $H\alpha$ spectral line very strongly. The patches of bright emission range in size from small areas which cover only a few millionths of the sun's visible disk, to great white filaments extending for over 12 000 million square km. Large flares are often accompanied by surge prominences to be described in the next section.

Flares are divided into three main classes - 1, 2, 3 according to their brightness and area, and using this system of classification a flare of importance 3 represents a very large, bright flare.

Flares are characterised by a very rapid rise to peak intensity followed by a slow decay. The development of a flare may be studied by observations of the $H\alpha$ line width, and is generally as follows:

(a) A sudden onset and rapid rise to peak brilliance, occurring within a few seconds.

(b) A period of maximum brightness which is usually over within four minutes.

(c) A slow decay in brightness of the flare, lasting from a few minutes for small flares to over an hour for larger ones.

It is generally believed that during the peak phase of the flare intense radio frequency and ultra-violet radiation is emitted. The ultra-violet radiation reaches the ionosphere at the same moment/.....

the same moment as $H\alpha$ emission becomes visible in a spectroheliosoope, and causes radio fade-outs and sudden changes in the earth's magnetic field.

At the time and place of a solar flare, the sun is believed to emit a cone-shaped beam of charged particles (mainly protons and electrons) which travels away from the sun with a velocity of approximately 1 600 km./sec. and reaches earth about 26 hours later. When this corpuscular stream reaches the ionosphere it causes a great disturbance of the earth's magnetic field (magnetic storm), gives rise to aurorae, and causes severe interference with radio communications.

(3) Filaments or Prominences

Prominences consist of chromospheric material extending into the corona. Two important types of prominence are described.

(a) Stationary Prominences

The existence of this fundamental type of prominence has been demonstrated by M. and Mme. d' Azambuja (1948). When fully developed it has the shape of a thin blade standing on edge, with an average height of 42 000 km., a thickness of only 6 600 km., and a length of 200 000 km.

Stationary prominences are sometimes observed to disintegrate in a spectacular manner. The prominence suddenly bursts upwards in the form of a great expanding arch, which rises to heights of hundreds of thousands of km. in the course of an hour or so. After this eruption, which seems to be a normal phase of evolution of this type of prominence, it may re-form in the position which it has already occupied for weeks.

These prominences are the most long-lived of solar surface markings, their duration being of the order of months.

(b) Surge Prominences Ellison (1949)

Surge prominences are short-lived jets of matter, ejected at the time of a solar flare, with velocities of about 100 km./sec. The matter rises to a height of about 100 000 km. and falls back along the same path.

C:/.....

TABLE 2/1 Smerd (1950)

THE ELECTRON DENSITY, ELECTRON TEMPERATURE, NATURAL FREQUENCY OF PLASMA OSCILLATIONS AND FREQUENCY OF ELASTIC COLLISIONS IN THE SOLAR ATMOSPHERE.

1	2	3	4	5	6
Distance from the sun's centre. Radius of the sun R_o = 6.95×10^5 $r = R/R_o$	Height above sun's surface. h (km.)	Electron density. N $(cm.)^{-3}$	Electron temperature ^oK	Natural plasma frequency f_o Mc./s.	Collision frequency. ν per sec. per electron
1.0	0	-	5.74×10^3	-	-
1.00072	5×10^2	5.72×10^{11}	1.70×10^4	6808.	6.47×10^6
1.00144	1×10^3	3.89×10^{11}	2.541×10^4	5615.	2.56×10^6
1.00288	2×10^3	1.80×10^{11}	3.0×10^4	3821.	9.69×10^5
1.00576	4×10^3	3.87×10^{10}	3.0×10^4	1769.	2.19×10^5
1.00864	6×10^3	8.29×10^9	3.0×10^4	819.3	4.94×10^4
1.0144	1×10^4	3.81×10^9	3.0×10^4 1.029×10^6	175.6	2.49×10^3 16.2
1.03	2.085×10^4	3.17×10^8	1.049×10^6	160.2	13.1
1.06	4.17×10^4	2.27×10^8	1.035×10^6	135.6	9.04
1.078	5.37×10^4	1.93×10^8	1.103×10^6	125.0	7.00
1.1	6.95×10^4	1.53×10^8	1.127×10^6	111.1	-
1.2	1.39×10^5	6.31×10^7	1.187×10^6	74.25	2.45
1.252	1.75×10^5	4.82×10^7	1.183×10^6	62.50	1.57
1.3	2.085×10^5	3.66×10^7	1.181×10^6	54.48	-
1.4	2.78×10^5	2.20×10^7	1.139×10^6	42.18	8.58×10^{-1}
1.5	3.475×10^5	1.41×10^7	1.082×10^6	33.75	-
1.6	4.17×10^5	9.40×10^6	1.017×10^6	27.60	4.39×10^{-1}
1.8	5.56×10^5	4.58×10^6	9.103×10^5	19.26	-
2.0	6.95×10^5	2.43×10^6	8.260×10^5	14.03	1.57×10^{-1}
2.2	8.34×10^5	1.37×10^6	7.467×10^5	10.53	-
2.4	9.73×10^5	8.11×10^5	6.852×10^5	8.11	7.04×10^{-2}
2.6	1.112×10^6	5.02×10^5	6.323×10^5	6.38	-
2.8	1.251×10^6	3.22×10^5	5.870×10^5	5.10	3.55×10^{-2}
3.0	1.39×10^6	2.23×10^5	5.235×10^5	4.25	-
3.5	1.738×10^6	8.43×10^4	4.728×10^5	2.61	1.31×10^{-2}
4.0	2.085×10^6	3.78×10^4	4.136×10^5	1.75	-
5.0	2.78×10^6	3.92×10^3	3.309×10^5	0.90	2.68×10^{-3}
6.0	3.47×10^6	3.32×10^3	2.755×10^5	0.54	1.19×10^{-3}
8.0	4.865×10^6	5.91×10^2	2.068×10^5	0.22	3.32×10^{-4}
10.0	6.255×10^6	1.55×10^2	1.655×10^5	0.11	1.23×10^{-4}

Note: The values of r, h, N, T and ν for f_o = 125 Mc./s. and 62.5 Mc./s were computed by the author, and will be referred to in subsequent chapters.

3: NUMERICAL DATA CONCERNING THE SOLAR ATMOSPHERE

An idealized form of the solar atmosphere, in which it is assumed to be a spherically symmetrical mass of fully ionized hydrogen, will be considered. The radius to the top of the photosphere is denoted by R_o, and a value of 6.95×10^5 km. will be used for this in numerical work. Points such as P in figure 2:1 are specified in terms of either their height "h" above the photosphere, or "r", where $r=R/R_o$, R being the distance from the centre of the sun. Table 2/1 compiled by Smerd (1950) lists various properties which are of importance in radio astronomy.

(1) The Electron Density

The electron density in the chromosphere is calculated for an exponential distribution after Gillié and Menzel (1935). It is given by

$$N = 5.72 \times 10^{11} \times e^{-7.7 \times 10^4 (h - 500)} \text{ electrons/(cm.)}^3$$

where h is the height above the photosphere in km.

Electron density in the corona is computed from the revised Baumbach formula - Allen (1947)

$$N = 10^8 (1.55\, r^{-6} + 2.99\, r^{-16}) \text{ electrons/(cm.)}^3 \qquad (2.1)$$

This formula for electron density distribution is based on optical observations taken over a number of years and at different phases of the solar cycle. It thus represents a space and time average of coronal electron density distribution.

(2) The Electron Temperature

An electron temperature of 3×10^4 °K has been deduced by Redman (1942) from observations of chromospheric emission line profiles. Redman's measurements refer to an estimated height of 1 500 km., and he suggests that the electron temperature would be about the same at higher levels in the chromosphere.

Coronal temperatures may be obtained from Alfven's (1941) formula for the temperature of an atmosphere under gravitational equilibrium, which in conjunction with the Baumbach- Allen

expression/.....

expression for electron density gives - Smerd (1950) -

$$T = 1.153 \times 10^{7} \frac{(0.221\, r^{10} + 0.176)}{(1.55\, r^{11} + 2.99\, r)} \ ^{o}K \qquad (2.2)$$

This formula results in a very nearly uniform temperature of 1×10^{6} ^{o}K throughout the inner corona. This value of electron temperature is in good agreement with the order of magnitude of temperature deduced from optical and radio observations. There is, however, a large degree of uncertainty in the present knowledge of the electron temperature in the solar atmosphere, especially for the transition from chromospheric to coronal temperatures, ... the temperature distribution outlined above should be regarded as an approximate representation only.

(3) The General Magnetic Field

There appears to be some doubt as to the constancy or even existence of a general magnetic field for the sun. Smerd (1950) assumes that the sun's magnetic field can be represented by an equivalent magnetic dipole at the centre of the sun, of moment 3.4×10^{18} oersted x $(\text{km.})^{3}$, and the positions of the levels of zero refractive index illustrated in figure 2:2 are found by using this value to compute the solar magnetic field.

D: THE DATA IN TERMS OF VARIABLES OF THE MAGNETO-IONIC THEORY

(1) The Physical Properties of the Solar Atmosphere in Terms of Frequencies

The physical properties of the solar atmosphere can be described in terms of three derived frequencies.

(a) The frequency, f_o, of plasma oscillations in the absence of a magnetic field given by

$$f_o^{2} = \frac{e^{2} N}{\pi m} = 81 \times 10^{6} N \ (\text{sec.})^{-2} \qquad (2.3)$$

where e is the electronic charge in e.s.u., and m the electronic mass in grams. It can be seen that f_o is a measure of the electron density.

(b) The electron/.....

(b) The electron gyro-frequency, f_H , defined by

$$f_H = \frac{e\,H}{2\pi mc} = 2.8 \times 10^6 \; H \; (\text{sec.})^{-1} \qquad (2.4)$$

where H is the magnetic field in oersted, and c the free space velocity of light. f_H is a measure of the magnetic field.

(c) The frequency, ν , of elastic electron-ion collisions per electron. Smerd and Westfold (1949) give the following expression for the collision frequency in the solar atmosphere:

$$\nu = e^4 N \left\{\frac{\pi}{2m(kT)^3}\right\}^{\frac{1}{2}} \ln (4kT/e^2 N^{1/3})^2$$

The logarithmic term is a slowly varying function of N and T, and can be taken as constant over large regions of the solar atmosphere. Mean values of 21 for the chromosphere and 31.5 for the corona are used in numerical work.

Hence, for the corona the following expression for the collision frequency is obtained:

$$\nu = 42 \, N \, T^{-3/2} \quad (\text{sec.})^{-1} \qquad (2.5)$$

(2) The Physical Properties for a Given Frequency

At any one wave frequency, f , it is convenient to express the physical properties of the solar atmosphere in terms of the dimensionless parameters **x**, y, z commonly used in magneto-ionic theory. These quantities are defined as follows:

$$x = f_o^2/f^2 \quad \text{i.e. proportional to N} \qquad (2.6)$$

$$y = f_H/f \qquad \text{proportional to H} \qquad (2.7)$$

$$z = \nu/2\pi f \qquad \text{proportional to } \nu \qquad (2.8)$$

These quantities, together with θ (the angle between the direction of propagation and the magnetic field intensity) uniquely define the possible propagation in the medium.

P.t.o.....

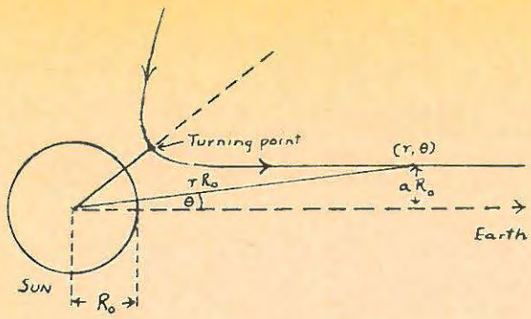

CO-ORDINATES SPECIFYING A RAY TRAJECTORY

PAWSEY AND SMERD (1953)

FIGURE 2:3

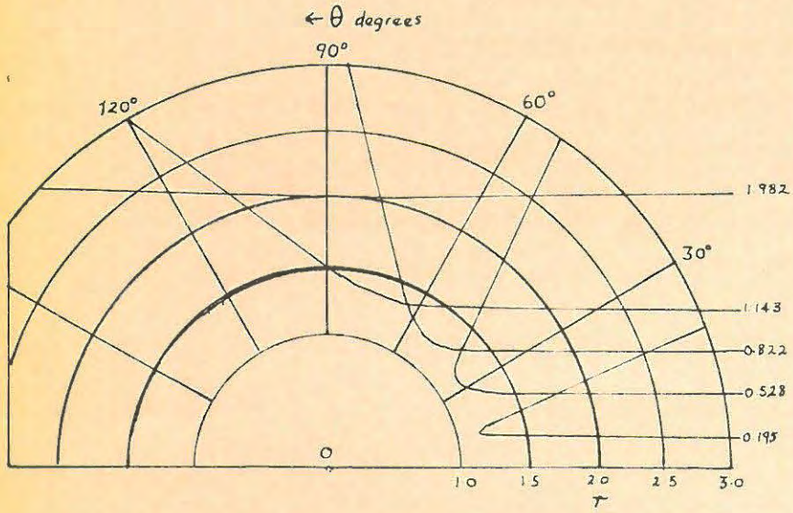

RAY TRAJECTORIES FOR 100 Mc/s; THE NUMBERS ON THE CURVES SPECIFY a. BOTH r AND a ARE IN UNITS OF THE RADIUS OF THE BASE OF THE CORONA, ASSUMED TO BE AT 10^4 km. ABOVE THE PHOTOSPHERE.

JAEGER AND WESTFOLD (1950)

FIGURE 2:4

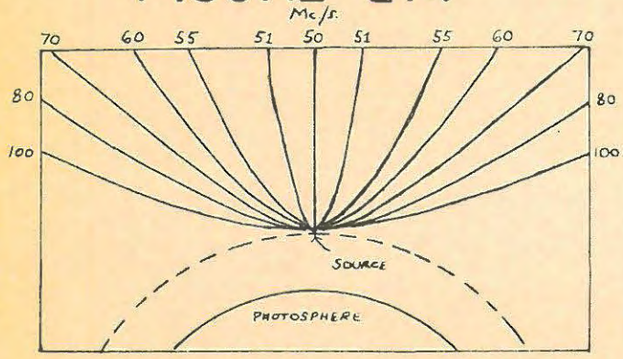

THE LIMITING RAYS OF OUTWARD EMISSION AT VARIOUS FREQUENCIES FROM A SOURCE AT THE 50 Mc./s. PLASMA LEVEL IN THE BAUMBACH - ALLEN CORONA.

WILD, MURRAY AND ROWE (1954)

FIGURE 2:5

E: RAY TRAJECTORIES IN THE SOLAR ATMOSPHERE

Because the refractive index varies throughout the solar atmosphere, ray paths may be curved. Typical trajectories have been computed by Jaeger and Westfold (1950).

Assuming a spherically symmetrical sun, the equation for a ray trajectory is

$$\theta = a \int_{r}^{\infty} \frac{dr}{r(\mu^2 r^2 - a^2)^{\frac{1}{2}}} \qquad (2.9)$$

where r, θ, are polar co-ordinates referred to the centre of the sun, "a" is the distance between the asymptote to the emerging ray and a parallel line through the centre of the sun (see figure 2:3), and μ is the refractive index at the point (r,θ). r and a are measured in terms of R_o, the radius of the photosphere.

The refractive index, μ, in the absence of magnetic fields is given from the Lorentz theory as:

$$\mu^2 = 1 - x \qquad (2.10)$$

and if N is known as a function of r, the trajectory for any given values of a and f may be constructed from these equations. Figure 2:4 illustrates typical ray trajectories for 100 Mc./s. radiation derived by Jaeger and Westfold (1950) by assuming the Baumbach-Allen formula for coronal electron density distribution.

In addition to causing bending of rays, refractive index variations selectively influence the velocity with which a disturbance is propagated. In an ionized medium the group velocity "u" is given by

$$u = \mu c \qquad (2.11)$$

where c is the velocity of light in free space, so that the total travel time is given by an integral of the form

$$t = \frac{1}{c} \int \frac{ds}{\mu} \qquad (2.12)$$

Numerical values for this integral in the solar atmosphere are given by Jaeger and Westfold (1950).

F:/.....

F: POINTS OF ZERO REFRACTIVE INDEX -- ESCAPE OF RADIATION

Points of zero refractive index occur in the solar atmosphere at $x = 1$ for the ordinary ray, and $x = 1 \pm y$ for the extraordinary ray. The inner of the two possible levels of zero refractive index for the ordinary ray (i.e. $x = 1 + y$) is usually neglected, since radiation emitted from this level encounters "stop bands" in propagation, and is not thought to be able to escape from the solar atmosphere. Figure 2:2 gives the height above the photosphere corresponding to zero refractive index for both the ordinary and extraordinary rays, and for different magnetic field conditions at selected frequencies.

The locus of points of zero refractive index for any given frequency defines a "shell" in the solar atmosphere. This shell gives both an inner limit from which a ray of that frequency generated in the solar atmosphere can escape, and an inner limit to which a ray can penetrate the solar atmosphere. Figure 2:5 shows the paths of rays of different frequencies escaping from a source at the 50 Mc./s. shell. The lowest frequency capable of escape is the plasma frequency itself, which can be propagated along the radial ray only. Higher frequencies can escape in directions contained within a sharply defined cone about the radial direction; the higher the frequency the wider the cone of emission. The lowest frequency capable of being received from a given level in the solar atmosphere by a terrestial observer is known as the critical escape frequency, f_c, which Smerd (unpublished data) has shown, in the case of the Baumbach-Allen corona, to be approximately related to the plasma frequency, f_o, at that level by the expression

$$f_c = f_o \sec (0.37\,\theta) \qquad (2.13)$$

for source angles, θ, between 0 and 80°, and frequencies between 20 and 100 Mc./s.

BIBLIOGRAPHY/.....

BIBLIOGRAPHY

Good accounts of solar physics relevant to radio astronomy are given by

SMERD, S. F. 1950 Proc. Instn. Elect. Engrs., 97, 447.

and in the following standard text-books on radio astronomy:

PAWSEY, J. L., BRACEWELL, R. N. 1955 Radio Astronomy, (Clarendon: Oxford)

KUIPER, G. P. (Editor) 1953 The Sun, (University of Chicago Press)

LOVELL, A. C. B., CLEGG, J. A. 1952 Radio Astronomy, (Chapman and Hall: London)

The numerical data quoted in this chapter concerning the solar atmosphere has been derived mainly from Smerd (1950).

CHAPTER THREE

GENERAL FEATURES OF SOLAR RADIO EMISSION AT METRE WAVELENGTHS

At metre wavelengths (frequencies below 300 Mc./s.) four distinct classes of solar radio waves can be distinguished.

(1) The Thermal Component.

(2) Enhanced Radiation.

(3) Outbursts.

(4) Isolated Bursts.

A: The Basic Thermal Component

Observations of radio waves at metre wavelengths received from the quiet sun show that they are of low intensity and are randomly polarized. The observed flux density and polarization are consistent with theoretical expectations for a thermal emission from the solar corona at a temperature of 10^6 °K.

B: Enhanced Radiation

This type of radiation is by far the greatest component of high intensity solar radio emission at metre wavelengths. It constitutes "noise storms" in which a high, but variable emission is maintained for hours or days on end.

Radiation at any one frequency appears as a slowly varying background level or "continuum" with frequent short-lived bursts superposed on it. The rise and fall of these bursts is often extremely rapid - much more so than the rise and fall of outbursts and isolated bursts.

The general properties of enhanced radiation on 97 Mc./s. have been determined by Payne-Scott and Little (1951) using a swept-lobe interferometer, which is capable of giving the location of rapidly moving radio disturbances and the instantaneous polarization of the radiation. Their results are summarized below:
(a) The radiation is circularly polarized, and the polarization of the short-lived bursts is usually of the same sense as that of the continuum.

(b)/.....

(b) The radiation is received from the direction of sunspot groups, and originates in an area of the sun of the same order of size as a visual sunspot.
(c) The sources of the enhanced radiation appear to lie high above sunspot groups, and do not show rapid movement.

The dynamic spectra of enhanced radiation were recorded by Wild and McCready (1950) using a swept frequency receiver operating in the frequency range 70-130 Mc./s. Their noise storm results have been analysed by Wild (1951). He noted that a relatively steady enhancement is often observed over a wide frequency range. In addition, short-lived, narrow band bursts which he calls storm bursts were observed superposed on the continuum. The instantaneous spectra of these bursts nearly always show the following features:
(a) A fairly symmetrical rise and fall.
(b) A narrow bandwidth - usually about 4 Mc./s. between points of $\frac{1}{2}$ maximum intensity.
(c) The mid-frequency of a burst remains approximately constant throughout its lifetime.

No detailed explanations of the origin of enhanced radiation have as yet been advanced, but the author is of the opinion that a synchrotron mechanism, to be described in Chapter Five, would account for the observed characteristics of storm bursts.

Storm bursts are classified by Wild and McCready (1950) as Spectral Type I.

C: Outbursts

Outbursts are marked increases in the intensity of solar radio noise which are closely associated with solar flares. They have been observed on frequencies between 9 and 35 000 Mc./s., but are particularly intense at metre wavelengths. At a single frequency outbursts appear as a sudden increase in intensity by

a factor/.....

a factor of thousands, a period of rapid fluctuation, followed by a gradual decay. They usually last for about 10 minutes, and are often followed by noise storms.

The statistical correlation between outbursts and flares has been investigated by Hey, Parsons, and Phillips (1948) on 70 Mc./s., and by Dodson, Hedeman, and Owren (1953) on 200 Mc./s. The former found that larger flares were more likely to be accompanied by a radio burst (50% of class 2 and 3 flares, 32% of class 1) ; the latter found a generally higher correlation (74% and 79% respectively).

Payne-Scott and Little (1952), observing on 97 Mc./s. with a swept-lobe interferometer, found that outbursts are always randomly polarized. They also found that the source position changed rapidly, and seemed in most cases to move from its initial position in the neighbourhood of a flare towards the sun's limb. They interpreted these changes in source position as the outward passage of an exciting source through the solar corona. By assuming that this exciting agency moved radially outwards from the flare, they found the source velocities to be in the range 500 - 3 000 km./sec.

The dynamic spectra of outbursts have been observed in the frequency range 70 - 130 Mc./s. by Wild and McCready (1950), and 40 - 240 Mc./s. by Wild, Murray, and Rowe (1954). Wild (1950a) and Wild, Murray, and Rowe (1954) have analysed these observations and find that the spectra of outbursts show the following distinguishing features:

(a) The peak intensity drifts slowly to lower frequencies, at a fairly constant rate of about 0.22 Mc./s. per second.

(b) Simultaneous duplication of features separated by a frequency range of about 2:1 is shown for about 50% of all bursts. The ratio of peak frequencies is often appreciably lower than, and never exceeds 2. Wild et al attribute this duplication to the emission of both fundamental and second harmonic frequencies

from a/.....

from a common source.

(c) The intensity of the second harmonic is comparable with, or greater than that of the fundamental; no third or fourth harmonics have been detected.

(d) Profiles of intensity versus frequency show that the fundamental peaks are markedly asymm etrical, the low frequency edge showing an abrupt cut-off. The harmonic band is more symmetrical, but on the average the low frequency edge is the steeper.

Wild et al suggest that radiation comprising an outburst is emitted in a band of frequencies about the natural plasma frequency f_o at the level of the source in the solar atmosphere. On this hypothesis the fundamental band is expected to be strongly attenuated on all frequencies below the critical escape frequency f_c - see Chapter Two - and the observed cut-off of its low frequency edge supports this idea. The drift of peak intensity towards lower frequencies is then explained as motion of the exciting source into regions of continuously decreasing electron density (i.e. the source moves outwards in the solar atmosphere), and by assigning the peak intensity on each frequency to a height in the solar atmosphere given by the Baumbach-Allen formula for coronal electron density distribution, Wild et al have calculated the radial components of outburst source velocities. They obtain values for this in the range 300 - 650 km./sec.

Outburst source velocities, deduced by Wild (1950a) from the rate of frequency drift, and by Payne-Scott and Little (1952) from directional observations of the solar disk, are of the same order of magnitude as those of the so-called auroral corpuscular streams which are believed to be omitted at the time of a solar flare, and it has been suggested that outbursts are caused by the passage of these streams through the solar atmosphere. Alternatively, Wild, Roberts, and Murray (1954) have suggested that outbursts may be caused by acoustic shock waves resulting from explosions in the inner regions of the solar atmosphere. These

waves/.....

waves would be propagated outward at the velocity of sound in the solar atmosphere, which is about 1 500 km./sec.

Outbursts, characterised by a slow drift in frequency towards lower frequencies, are classified by Wild and McCready (1950) as Spectral Type II.

D: Isolated Bursts

In addition to outbursts, other less intense, sporadically occurring bursts are often observed. These bursts, which tend to occur in groups, are not circularly polarized, and are of much shorter duration than outbursts. They were called isolated bursts by Pawsey (1950) because they were first regarded as occurring isolated from noise storms, and unpolarized bursts by Payne-Scott (1949) who used this feature to identify them even in the presence of noise storms. Loughhead, Roberts, and McCabe (1957) report that there is a high degree of association of isolated bursts with minor flares (mainly microflares: class 1^-) and that these flares are approximately uniformly distributed across the solar disk.

Single frequency observations of isolated bursts show that the intensity rises fairly sharply to a maxim um value, and then decays more gradually to the original level, the whole process occupying a few seconds. Isolated bursts on frequencies of 85, 65, 60, and 19 Mc./s. have been studied by Payne-Scott (1949) and the following characteristics were noticed:

(a) The bursts tend to occur very nearly simultaneously over the range of frequencies, and usually arrive in the order of decreasing frequency.

(b) On any given frequency the decay portion of the burst profile appears to be exponential.

(c) Double-humped bursts are common.

The dynamic spectra of isolated bursts have been observed by Wild (1950b) in the frequency range 70 - 130 Mc./s., and by Wild, Roberts, Murray (1954), Wild, Murray, and Rowe (1954) in the frequency range 40 - 240 Mc./s.

The spectra/.....

The spectra have much in common with those of outbursts, and their main features are summarized below:

(a) The peak intensity drifts rapidly to lower frequencies at a rate of approximately 20 Mc./s. per second, and the rate of frequency drift appears to decrease with time. Often, the rate of drift is observed to decrease so rapidly that the emitted peak becomes almost "stopped" at a fixed frequency.

(b) The spectral features of isolated bursts are commonly duplicated, the frequency ratio of the peaks being about 2:1. Once again, this duplication of features is attributed to the emission of fundamental and second harmonic frequencies from a common source. Comparison of the instantaneous profiles of the two bands normally indicates that the low frequency edge of the fundamental band has been cut off during escape.

On the same assumptions that were made in the case of outbursts, Wild (1950b) has derived the radial components of isolated burst source velocities, and obtains values in the range $2 \times 10^4 - 10^5$ km./sec. In some cases the source velocity appears to increase or remain approximately constant in its passage outwards through the corona, but most commonly the source is found to decelerate.

Wild, Roberts, and Murray (1954) suggests that these bursts are excited by fast moving particles ejected from the sun at the time of a solar flare. They point out that particles travelling with velocities of 5×10^4 km./sec. would reach earth about 50 minutes after the onset of a flare. This time interval is typical of the delays observed between solar flares and increases in cosmic ray intensity which sometimes accompany them, and it is therefore possible that isolated bursts are caused by high energy cosmic ray particles. Particle velocities of this magnitude have not been observed in the solar atmosphere, but, even if present, they might well escape optical detection.

Sporadic bursts characterised by rapid frequency drift to lower frequencies are designated as Spectral Type III.

TABLE 3/1

Wild and McCready (1950)

CLASSIFICATION OF BURSTS OF SOLAR RADIATION AT METRE WAVELENGTHS

Class of Burst. Spectral Type.	Occurrence	Polarization	Visual Correlation.	DYNAMIC SPECTRUM		
				BANDWIDTH	DURATION	REMARKS
Storm Bursts I	Noise Storms	Circular	Sunspots	Narrow	Seconds	No frequency drift
Outbursts II	Sporadic	Not circular	Flares	Broad	Minutes	Complex profiles. Slow drift to lower frequencies
Isolated Bursts diverse including III	Sporadic	Not circular	Flares* esp. micro-flares	Broad	Seconds	Type III bursts show rapid drift to lower frequencies

* This has been inserted by the author in view of the results of Loughhead et al (1957).

(1). Large Outburst. Dec. 19 1957.

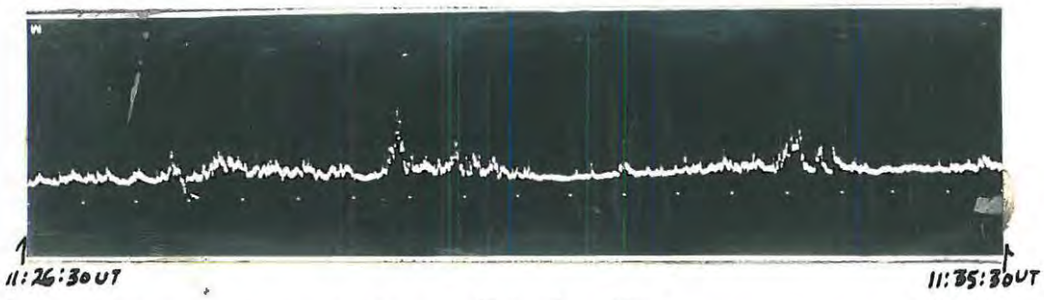

(2) Enhanced Radiation. Feb. 6 1958.

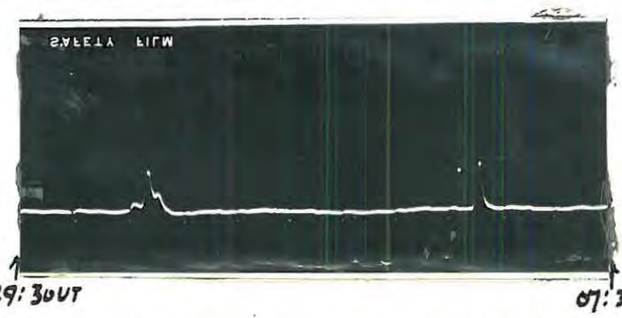

(3) Double-humped and simple isolated bursts. Jan. 24 1958.

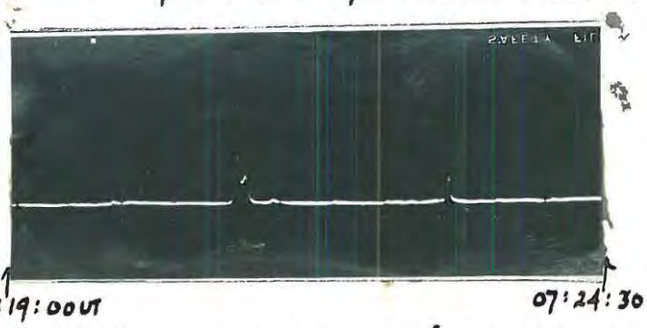

(4) Double-humped and simple isolated bursts. Feb. 3 1958.

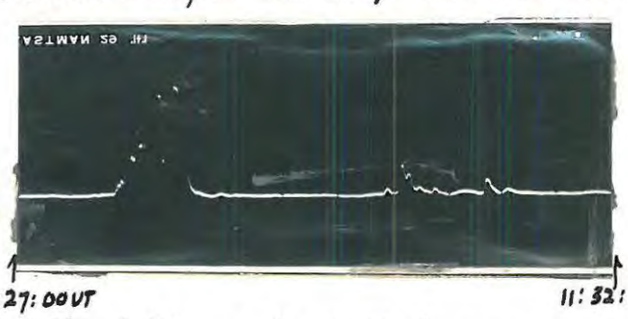

(5) Outburst followed by double-humped and simple isolated bursts. Jan. 24 1958.

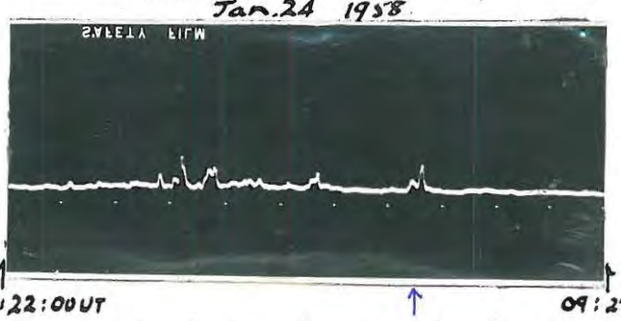

(6) Reversed double-humped burst. Jan. 23 1958.

PLATE D. Typical "bursts" of solar radio noise recorded by the Rhodes University equipment at a frequency of 125 Mc/s.

E: Typical Solar Burst Profiles on 125 Mc./s.

Plate D de picts intensity-time profiles of various bursts received by the Rhodes University equipment on a frequency of 125 Mc./s. during the period November 26 1957 - February 6 1958.

(1) One of the largest outbursts recorded by the equipment, which occurred on December 19 1957, is shown. The main phase of the outburst lasted from (08:02:30 U.T.)—(08:10:00 U.T.). According to the "Daily Maps of the Sun" issued by the Fraunhofer Institute, a flare of importance 2+, heliographic co-ordinates 19°N, 15°E, is reported to have occurred over this period, and it seems very probable that this flare and outburst are associated.

(2) This print illustrates enhanced radiation, observed on February 6 1958, which constituted part of a noise storm recorded on February 6, 7, &8. The steadily varying enhanced base level (continuum) and rapidly fluctuating storm bursts are clearly depicted.

(3) & (4) Double-humped isolated bursts followed by single peaks are shown. Features to notice are the smooth profiles, rapid rise, and more gradual decay.

(5) An outburst followed by an isolated burst is shown. From this record an idea of the relative intensities of outbursts and isolated bursts may be obtained.

(6) A "reversed" double-humped burst, which is more or less a mirror image of the double-humped bursts commonly observed, is shown. Only two well-defined reversed bursts were recorded in the period considered, as against about 20 "normal" double-humped bursts.

BIBLIOGRAPHY

Excellent reviews of solar radio emission are given in the following books:

PAWSEY, J. L., BRACEWELL, R. N. 1955 Radio Astronomy, (Clarendon: Oxford)

KUIPER, G. P. (Editor) 1953 The Sun, (Univ. of Chicago Press)

CHAPTER FOUR

ISOLATED BURSTS

(Observations and results from previous investigations)

A summary of the characteristics of isolated bursts, as reported by previous investigators, is given in the following pages.

A: Williams (1948) Single frequency receiver 75 Mc./s.

99 isolated bursts, each lasting a few seconds, were observed using a receiver with a linear power gain. An analysis of the "tails" of 78 of these bursts was made; 21 were not analysed because the height of the pulse peak was less than 25% of the background value, and too short a length of falling slope was available for significant measurements to be made. Of the 78 bursts analysed, the tails of 58 were found to be very probably exponential in shape, 11 less probably so, 4 probably not so, and 5 definitely not so.

Typical Burst Shape

Between 3/4 and 9/10 of the broken line in the above figure was analysed for each burst, and the deviation from average of the factor k in exp (-kt) was less than ± 15% for any burst assumed to have exponential form. Expressing Williams's "half-life" values in terms of k gives a most common value of k = 0.7 sec.$^{-1}$, with a range from 0.3 to 1.8 sec.$^{-1}$

Williams considered that consecutive bursts, which presumably came from the same region in the solar atmosphere, should have the same half-life. His results, however, do not confirm this.

Attempts by Williams to interpret the rising portion of

burst profiles/.....

burst profiles in terms of exponential functions were not successful.

B: Payne-Scott (1949)

Single frequency receivers 85, 65, 60, &19 Mc./s.

(1) Polarization

Payne-Scott found that isolated bursts were not circularly polarized. Their polarization must therefore be either plane or random.

(2) Relative Intensities at Different Frequencies

Observations of corresponding bursts on 60 and 85 Mc./s. showed that the lower frequency normally had the higher intensity, the average ratio of peak intensity on 60 Mc./s. to that on 85 Mc./s. being about 2 to 1 - approximately the square of the corresponding wavelengths.

(3) The Profiles of Isolated Bursts

Typical isolated bursts showed a finite rise time, rounded top, and more gradual decay, reminiscent of the transient response of a medium possessing a resonant frequency. On the assumption that the decay rate was a characteristic of the medium rather than of the initiating disturbance, the decay rates of 100 isolated bursts on 85 and 60 Mc./s. were measured . The base level was taken as the level before a burst appeared. The decaying portion of burst profiles was found to fit very well a curve of the form

$$I = I' \text{Exp}(-kt)$$

where I was the power incident upon the antenna. For both frequencies a fairly symmetrical distribution of k was found, about a median value of 0.6 sec.$^{-1}$ k was also measured for a few bursts on 19 Mc./s., and was found to be about 0.25 sec.$^{-1}$

Payne-Scott reports one further feature of burst shapes. Single peak bursts were found to be much less common than double-

humped/.....

humped bursts. The ratio of intensity of the two peaks was about 4 to 1 on both 60 and 85 Mc./s., the first peak being larger in nearly every case. The time interval between the peaks was in the range 2 -- 10 seconds. Measurements of the decay rates of the first peaks of double-humped bursts suggested that they decayed more rapidly than single peak bursts. Measurements of k on 125 Mc./s. by the author - see Chapter Six - are in agreement with this result.

(4) Time Delays between the Arrival of Corresponding Bursts on Different Frequencies.

Isolated Bursts usually arrived in the order of decreasing frequency. The time delay between the start of a burst on 85 Mc./s. and on 60 Mc./s. varied between 0 and 1.5 seconds, with a most common value of 0.7 seconds. Corresponding delays between 65 and 60 Mc./s., and 60 and 19 Mc./s. were 0.3 and 9 seconds respectively.

Assuming that radiation is excited at levels of zero refractive index in the solar corona by outward moving sources, the author has calculated the radial source velocities corresponding to Payne-Scott's observed delay times for the above three cases.

Frequency Interval	Distance between Levels of Zero Refractive Index	Delay Time	Source Velocity
Mc./s.	km.	secs.	km./sec.
85--60	0.71×10^4	0.7	1.0×10^4
65--60	0.19×10^4	0.3	0.6×10^4
60--19	37.1×10^4	9.0	4.1×10^4

These derived velocities are in fairly good agreement with one another, and with Wild's (1950b) results of 2×10^4 - 10^5 km./sec. This table appears to indicate that burst sources accelerate in their outward passage through the solar atmosphere, but does not offer positive evidence for this, since if the source decelerated it might well become stopped before reaching the 19 Mc./s.

level/.....

DYNAMIC SPECTRA OF ISOLATED BURSTS

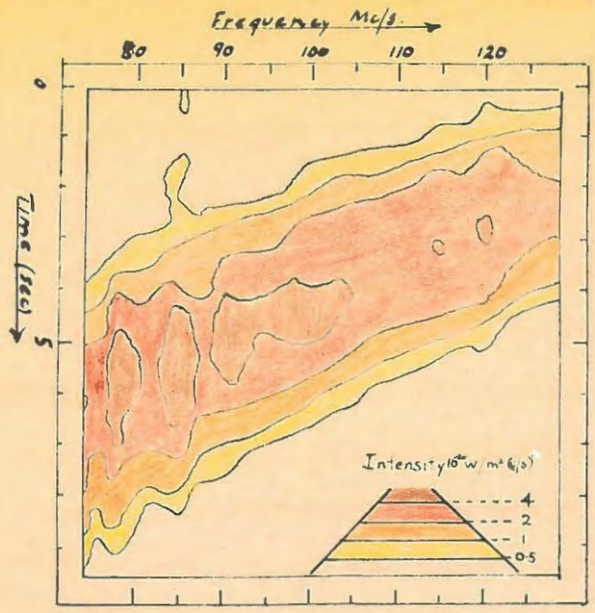

Type III Burst. Wild (1950b)

FIGURE 4:1

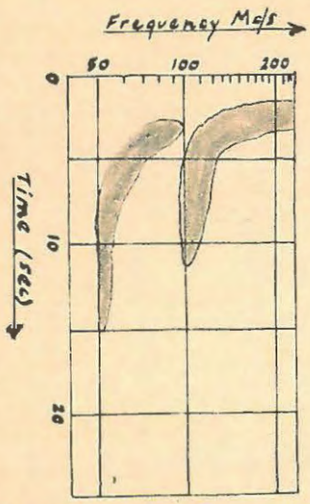

Harmonic Pairs in Type III spectra.
Wild, Murray, and Rowe (1954)

FIGURE 4:2

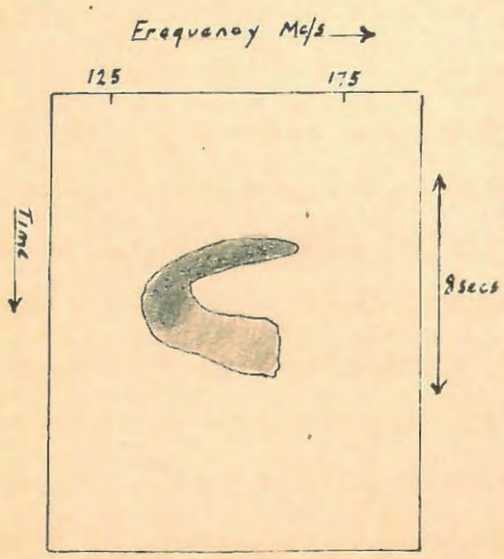

U Burst. Maxwell and Swarup (1958)

FIGURE 4:3

level, and hence decelerating sources would not necessarily contribute to the above readings.

C: Wild (1950b) Swept frequency receiver 70--130 Mc./s.

The dynamic spectra of isolated bursts were observed using a swept frequency receiver. One sweep of the band occupied 0.07 seconds, and the band was swept about 3 times per second. As the receiver swept the frequency band, the output was displayed as an intensity modulated spot moving in the Y-direction on a cathode ray tube screen. This was photographed on film moving slowly in the X-direction, producing a frequency-time record with solar intensity appearing as variations in photographic density. The dynamic spectrum of a fairly simple isolated burst is shown in figure 4:1.

(1) DESCRIPTION AND CHARACTERISTICS OF OBSERVED SPECTRA

a) Frequency and Time Profiles

A horizontal cross-section of a burst "contour diagram" depicting the variation of intensity with frequency at a particular time is referred to by Wild as a frequency profile. Similarly, a vertical cross-section depicting the variation of intensity with time at a particular frequency is referred to as a time profile.

Frequency profiles of isolated bursts were usually fairly smooth curves, with no sudden variations of intensity within frequency intervals of the order of a few megacycles per second. The bandwidth of the frequency profiles, measured between points of $\frac{1}{4}$ maximum intensity, was rarely less than 10--15 Mc./s., and often very much greater. In simple cases the frequency profiles showed only one maximum. Such profiles were generally unsymmetrical, and the variation of intensity with frequency on the low frequency side of the maximum tended to be greater than that on the high frequency side. In other cases, such as that illustrated in 4:1, frequency profiles often showed more than one maximum.

The time/.....

The time profiles of simple isolated bursts were similar to those observed by Williams (1948) and Payne-Scott (1949), and showed a gradual rise to maximum intensity, followed by a more gradual decay to the original level. Profiles of more complicated isolated bursts showed several maxima. On the average about 60% of the total lifetime of a burst was spent in decay, and the decay was approximately exponential. Once again, this is in agreement with the results of Williams and Payne-Scott.

(b) Groups of Bursts and Complex Bursts

Although isolated bursts sometimes occurred as single disturbances preceded and followed by quiet periods of several hours duration, they were frequently found to occur in small groups of two or three bursts arriving in rapid succession. This effect led Wild to suggest that isolated bursts with complex spectra may in fact be caused by clusters of superimposed simple bursts. This interpretation is supported by the fact that portions of complex bursts often appeared to resemble typical kinds of simple bursts.

(c) Energy Spectra

Wild obtains the result that the energy of isolated bursts, determined by graphical integration of the time profiles, increased greatly with decreasing frequency. This result is consistent with that of Payne-Scott (1949).

(d) Variation of Frequency Profiles with Time

The frequency profiles of simple bursts, having a single maximum value, usually changed with time in one of two ways.

(i) The peak frequency remained approximately constant throughout the lifetime of a burst.

(ii) The peak frequency drifted rapidly with time, almost always in the direction of decreasing frequency. The rate of drift seldom differed from an average value of about 20 Mc./s. per second by a factor of more than 2. These bursts represented the majority of isolated bursts observed, and Wild and McCready (1950) have classified them as spectral Type III.

(2)/.....

(2) TYPE III BURSTS

20 Type III bursts were recorded, but only about a half of these were sufficiently well defined for useful analysis. Their characteristics are described below.

(a) Lifetime and Bandwidth

The lifetime at any one frequency tended to increase slightly with decreasing frequency for most bursts. The mean lifetimes for the Type III bursts considered (measured between points of $\frac{1}{4}$ maximum intensity) ranged between 2.9 and 3.8 seconds. Bandwidths, measured on the frequency profiles, were usually greater than 50 Mc./s.

(b) Decay Constant

The decay of Type III bursts, as observed on time profiles, was found to be approximately exponential in form, and could be represented by the relation

$$I = I' \exp(-kt)$$

Wild obtained values of k on 100 Mc./s. for 10 bursts, which ranged from 0.6 - 1.5 sec.$^{-1}$, with a mean value of 1.0 sec.$^{-1}$ Values of k for other types of isolated bursts were sometimes a little less.

Of 12 Type III bursts considered suitable for analysis, 5 exhibited a steady decrease of k with decreasing frequency, 2 more suggested a decrease of k with decreasing frequency, and the remaining 5 were inconclusive. Wild (1950b:Fig.4) plotted a graph of the normalized decay constant $k/\bar{k}$ (averaged over these 12 bursts) versus frequency, where $\bar{k}$ is the mean value of k over the frequency range for a single burst. This graph was a straight line through the origin, and Wild therefore suggested that the decay constant in the frequency range considered could approximately be represented by

$$k = K f \qquad (4.1)$$

where K is a constant (of the order of 10^{-8}) for a given burst.

(c)/.....

(c) Frequency Drift

The locus of points of maximum intensity on the frequency - time plane of burst contour diagrams is referred to as the ridge line. The drift rate is defined by Wild as the rate of change of frequency with time along the ridge line. In all well defined cases, the drift rate became slightly slower as the frequency decreased.

Wild found that the negative drift rate could approximately be represented by a single power function of frequency:

$$-\frac{df}{dt} \propto f^n \qquad (4.2)$$

where f and t specify points on the ridge line of a given burst. He pointed out that if the Baumbach-Allen coronal electron density distribution was assumed, the drift rate for a source moving outwards at constant velocity would be given by putting $n \doteq 1.5$ in equation (4.2). Values of $n < 1.5$ would imply an accelerating source, and $n > 1.5$ a decelerating source. The observed values of n for the Type III bursts considered varied between 0.5 and 1.5 (implying a slight acceleration of source) with a mean value of about 1.0, which gave the result that the negative drift rate is approximately proportional to frequency:

i.e.

$$-\frac{df}{dt} = \frac{f}{a} \qquad (4.3)$$

where a is a constant (of the order of a few seconds) for a given burst.

(d) Derived Source Velocities

Wild suggests that frequency drifts may be caused by outward moving disturbances in the solar atmosphere. If radial source velocities are calculated by assigning each frequency to its zero refractive index level, the resulting values obtained by Wild corresponding to the observed drift rates are in the range 2×10^4 — 10^5 km./sec. The slight discrepancy between these values and those derived by the author from Payne-Scott's results may

be duo/.....

be due to the fact that Payne-Scott measured time delays between the start of corresponding bursts on different frequencies, whereas Wild measured the time delays between corresponding peaks.

D: Wild, Murray, and Rowe (1954)

Wild, Roberts, and Murray (1954)

Swept frequency receiver 40 - 240 Mc./s.

(1) NEW FEATURES IN THE SPECTRA OF TYPE III ISOLATED BURSTS

The greater frequency range of this apparatus revealed new features in the spectra of Type III bursts.

(a) Drift Rate

The rate of drift was often observed to decrease so rapidly, that at the lower frequencies the emitted peak became almost "stopped" at a fixed frequency. The observed drift rates appeared to indicate that in most cases the source decelerated in its outward passage through the solar corona. N.B. This result is not in agreement with Wild's (1950b) result reported above.

(b) Harmonic Emission

(i) Bursts frequently appeared in "harmonic pairs", in which the spectral features of a burst were duplicated at about double the frequency. This duplication is attributed to the emission of fundamental and second harmonic frequencies from a common source. The dynamic spectrum of a harmonic pair is shown in figure 4:2.

(ii) Bursts showing detectable fundamental and second harmonic emission accounted for a considerable proportion (perhaps 50% or more) of all bursts observed.

(iii) The intensity of the second harmonic was of the same order of magnitude as that of the fundamental. No higher harmonics were detected. If they had been present, with an intensity one-tenth of that of the second harmonic, they would almost certainly have been detected.

(iv) The instantaneous ratio of peak frequencies varied in most cases between 1.35 and 2, and never exceeded 2.

(v)/.....

(v) Comparison of the instantaneous frequency profiles of the fundamental and harmonic bands showed that in all cases they were similar in shape. Usually, however, the low frequency edge of the fundamental band appeared to have been cut off during escape. Wild, Roberts, and Murray claim that this result justifies the assumption made in calculating source velocities that radiation observed on any one frequency originates at the level of zero refractive index in the solar atmosphere for that frequency.

(2) COMPOUND BURSTS

It is well known that Type II outbursts and Type III clusters may occur at the time of a solar flare. Either kind may occur without the other, but on three occasions Wild, Roberts, and Murray have observed a combination of the two types of event. In each case the Type II outburst followed the Type III cluster after a time delay of several minutes. Wild, Roberts, and Murray (1954:Fig.3) plotted a graph of derived height in the solar atmosphere versus time for the Type II outburst and Type III cluster in each case. They found that although the derived velocity and time delay of the Type II outburst differed considerably in each of the three cases considered, the velocity lines of the Type II outburst and Type III cluster, when extrapolated towards the origin, yielded in each case a point of intersection in the lower corona, within 10^5 km. of the photosphere. This result led Wild et al to suggest that the two events comprising a compound burst were associated with disturbances, perhaps streams of matter, ejected simultaneously from a common source situated low in the solar atmosphere. This "source" could in fact be the primary cause of a solar flare.

E: Loughhead, Roberts, and McCabe (1957)

Swept frequency receiver 140 - 240 Mc./s.

The relationship of Type III bursts to solar flares was investigated by comparing simultaneous radio and optical observations. Over 300 flares were examined, 85% of which were micro-

flares/.....

flares (class 1⁻). A summary of the results obtained is given below:

(1) About 20% of the flares were associated with Type III bursts, whereas more than 60% of the bursts occurred during the lifetime of a flare.

(2) The association of bursts and flares was independent of the positions of flares on the solar disk, apart from an apparent deficit for flares on the western hemisphere more than 30° from the central meridian. The occurrence of Type III bursts over a wide range of disk longitudes seems to imply a wide cone of emission of Type III radiation.

F: Maxwell and Swarup (1958)

Maxwell, Swarup, and Thompson (1958)

Swept frequency receiver 100 - 580 Mc./s.

Recent observations of the dynamic spectra of solar bursts by these investigators have shown that Type III bursts tended to occur in groups - cf. Wild (1950b). They give the derived velocities of Type III burst sources as about 3×10^4 km./sec., and this is also in good agreement with Wild's (1950b) results. In addition they have discovered a new type of fast-drift burst which on their records appears in the form of an inverted "U". The dynamic spectrum of a typical U burst is illustrated in figure 4:3. U bursts were a relatively uncommon phenomenon, and accounted for only about 5% of all fast-drift bursts observed. The dynamic spectra of U bursts showed that the peak intensity drifted rapidly to lower frequencies with time, until it became stationary at a particular frequency in very much the same manner as a "normal" Type III burst. However, after reaching this particular frequency, the peak intensity was then observed to drift towards higher frequencies again. The duration of 43 U bursts observed was between 3 and 10 seconds. U bursts were usually found to be associated with flares (particularly microflares), and the percentage of U bursts that occurred at the time of a

flare/.....

flare is about the same as the percentage of normal Type III bursts that occurred during flares.

G: Wild and Sheridan (1958)

Swept frequency interferometer 40 - 70 Mc./s.

Wild and Sheridan describe a new type of instrument suitable for the study of solar bursts at metre wavelengths - a swept frequency interferometer. This instrument is capable of measuring the one-dimensional position and angular size of a transient source on the solar disk, and the polarization and intensity of the received radiation. All these characteristics are determined as a function of frequency in the range 40-70 Mc./s.

Some preliminary results for Type III burst sources were obtained using this instrument:

(1) The angular size of Type III burst sources remained approximately constant throughout the lifetime of an individual burst at any one particular frequency.

(2) On the average the angular source size was found to increase from about 6 minutes of arc at 65 Mc./s. to 10 minutes of arc at 45 Mc./s. An idea of the extent of Type III burst sources can be obtained by comparing these values with the angular size of the sun's visible disk, which is 32 minutes of arc.

The result that the source size increases with decreasing frequency has led Wild and Sheridan to suggest that the emitting region in the solar atmosphere could be cone shaped, the diameter increasing with height. The author has calculated the height in the solar atmosphere of the apex of this cone, making the usual assumptions of Baumbach-Allen conditions, and outward moving sources generating radio waves at levels of zero refractive index. The apex of the cone turned out to be at a height of 1.5×10^4 km. above the photosphere, corresponding to the level of zero refractive index for 170 Mc./s., and it seems reasonable to identify this height with the location of the primary disturbances which give rise to Type III events. This result is in good agreement with those obtained by Wild, Roberts, and Murray (1954) from a study of compound bursts. The height of the primary disturbance for one particular compound event is given by them (1954:Fig.3) as 3×10^4 km. above the photosphere, corresponding to the 150 Mc./s. level.

.....

The author believes that the above reports comprise all the published observations on isolated bursts up to the time of publication of this thesis.

CHAPTER FIVE

MECHANISMS OF ORIGIN OF ISOLATED BURSTS

Although the profiles and lifetimes of isolated bursts indicate that a transient disturbance in the solar atmosphere is involved, little is known of the way in which such bursts arise. Any suggested mechanism must be able to account for the following observed characteristics, viz:

(1) Electromagnetic radiation is generated in a localized region above the solar disk.

(2) Second harmonic emission is common.

(3) The radiation is able to escape from the solar atmosphere.

(4) The intensity of the received radiation is about 500 times that of the thermal emission from the quiet sun.

(5) The frequency of maximum intensity drifts rapidly to lower frequencies.

(6) The received radiation is not circularly polarized.

It does not seem likely that isolated bursts are of thermal origin, because to account for the observed intensities it is necessary to postulate temperatures of the order of 10^{10} ^{o}K in localized regions of the corona. In addition, it is difficult to see how any thermal process could result in harmonic emission.

The present trend is to explain solar bursts in terms of one of two processes, each of which, in principle, is capable of accounting for their observed properties.

(a) Oscillations at the electron gyro-frequency.

(b) Magnetohydrodynamic, or hydromagnetic waves.

The fundamental physical ideas involved, and suggested models to account for isolated bursts, will be discussed for each process.

A: Oscillations at the Electron Gyro-Frequency

The emission of radio frequency bursts is considered to be due to a radiation process similar to that observed in

synchrotrons./.....

synchrotrons. The electron gyro-frequency is given by

$$f_H = \frac{e H}{2\pi mc} \qquad \text{see equation} \qquad (2.4)$$

from which it may be verified that magnetic fields of 20 to 40 oersted are required for the generation of frequencies in the range 50 - 200 Mc./s.

Schwinger (1949) has shown that electrons oscillating at the gyro-frequency can produce harmonics. Kruse, Marshall, and Platt (1956) have shown that electrons rotating with non-relativistic velocities in a localized region would be capable of emitting radio waves with the observed intensities. A simple model of isolated bursts after Kruse et al is as follows:

Jets of electrons spiral outwards from sunspots around the lines of force of sunspot magnetic fields. They emit a spectrum consisting of lines which are harmonics of the fundamental gyro-frequency, and all components of the line spectrum decrease in frequency as the electrons move into regions of decreasing magnetic field. Furthermore, if the electron velocity is small compared with that of light, the intensity of the third harmonic is very much less than that of the fundamental and second harmonic, in agreement with observations.

There are, however, two grave objections to this model.
(a) Most authors - e.g. Ryle (1948) - are of the opinion that the fundamental frequency of synchrotron radiation is not able to escape from the solar atmosphere.
(b) Even if escape is possible, the polarization of received radiation is expected to be elliptical in general.

These objections are interrelated and will be considered together. Ryle argued that synchrotron radiation was produced only in the extraordinary mode of the magneto-ionic theory. Reference to figure 5:1 shows that, in order to escape, radiation propagating in the extraordinary mode has to pass through regions where the refractive index, n , is largely imaginary - stop bands -

and consequently/.....

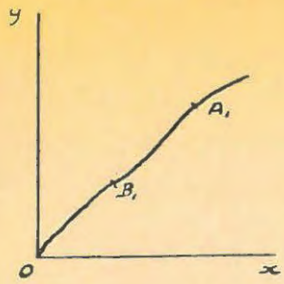

The escape of radiation from a mass of ionized gas may be conveniently studied with the aid of (x, y) diagrams of the type shown. The point A_1 has coordinates x_1 and y_1, which are the values of the x and y parameters of the magneto-ionic theory at the corresponding point A in the gas. If x and y change continuously in the gas, a ray trajectory, say AB can be represented in the diagram by the continuous curve A_1B_1. If the ray passes out of the body, the corresponding curve A_1B_1 approaches the origin and reaches it when the ray finally emerges from the body and its associated magnetic field.

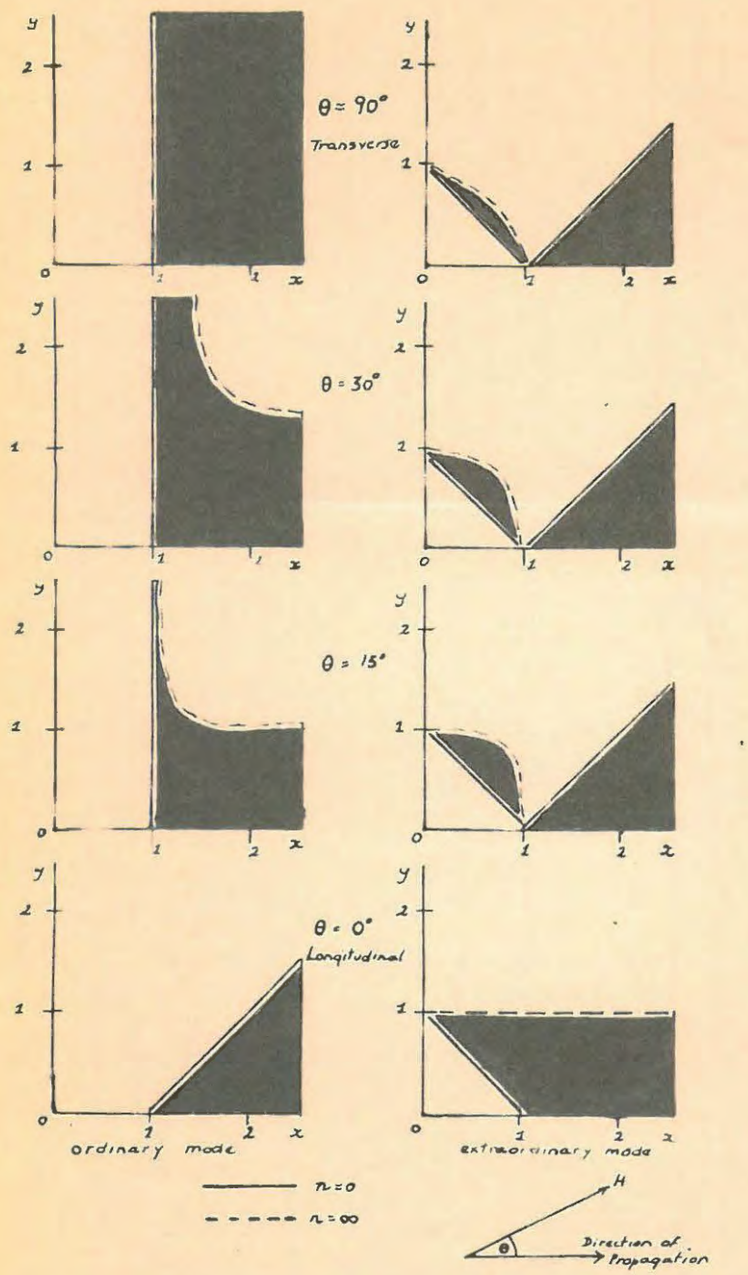

"Pass" and "Stop" (shaded) regions for the ordinary and extraordinary magneto-ionic modes for various angles θ – reproduced from Pawsey and Bracewell (1955: Fig. 39)–. From these diagrams it may be seen that synchrotron which originates at $y = 1$ encounters stop bands in all cases when propagating in the extraordinary mode, and that escape is only possible for radiation propagating in the ordinary mode if it originates in a region where $x < 1$.

FIGURE 5:1

and consequently such radiation would be completely absorbed. However, Kruse et al point out that synchrotron radiation can in general propagate in both the ordinary and extraordinary mode. As before, the extraordinary mode cannot escape the solar atmosphere. If $x = f_o^2 / f^2 > 1$ the ordinary mode encounters a stop band at $x = 1$ and cannot escape, but if the radiation process takes place in a region where $x < 1$ the ordinary mode can escape. According to Ryle's calculations, it appears that magnetic fields necessary for generation of 50 - 200 Mc./s. radiation can be maintained in regions of the solar atmosphere where $x < 1$, above sunspots with magnetic fields of the order of 3 000 oersted at the photosphere. Consequently radiation propagating in the ordinary mode can sometimes escape. According to Pawsey and Bracewell (1955:Fig.39) such radiation is in general elliptically polarized, tending to circular when the magnetic field is in the direction of propagation, and plane for a transverse magnetic field.

Payne-Scott's (1949) observations show that received radiation is either plane or randomly polarized, and on these grounds it seems unlikely that synchrotron emission is responsible for isolated bursts.

Nevertheless, solar radiation showing circular or elliptical polarization may be caused by synchrotron radiation, and for this reason the author suggests that noise storm bursts, and possibly the associated enhanced continuum may originate in a synchrotron type process. Furthermore the author considers that synchrotron emission provides a natural explanation for the U bursts described by Maxwell and Swarup (1958). Their frequency drift may be explained in terms of electrons gyrating along a line of force above a bipolar sunspot into regions of decreasing magnetic field, and then being guided back to regions of increasing field. On such a hypothesis the observed polarization is expected to be circular at the start of such a burst, and become increasing elliptical until the turning point was reached. The

polarization/.....

polarization would then be plane. After the turning point the polarization would again become elliptical, tending to circular with time. No observations have as yet been made on the polarization of U bursts, so that it is not possible at present to say whether this model is correct.

B: Magnetohydrodynamic, or Hydromagnetic Waves

The generation of electromagnetic radiation in an electrically neutral, highly ionized gas - a plasma - is attributed to the various types of wave that can exist in the medium. A complete non-linear theory of strong waves is very complex, so that attention is usually confined to weak waves, which provide an insight into the physical mechanisms occurring. Piddington (1955) has shown that there are only 4 possible weak waves in a plasma. These are two shear type magnetohydrodynamic waves described by Alfvén (1950), which have been called the "O" and "E" waves, a plasma "P" wave, and a magnetic sound "S" wave.

The O and E waves are so named because they correspond to the O and E radio waves. In fact the latter are the simpler limiting cases at frequencies so high that the heavy ion motion is negligible. The gas always moves in a direction perpendicular to the magnetic field suggesting the description "shear waves", and there are no local excesses in density of electrons or positive ions, and hence no space charge effects.

The plasma, or P wave is associated with the presence of space charge and consequent coulomb forces. If a plasma is perturbed so as to produce small local excesses of electrons or positive ions, after removal of the impressed force the space charge simply oscillates at a frequency characteristic of the medium. To illustrate this, the simple case of linear oscillations of electrons in a uniform, fully ionized medium with no external magnetic field is considered. The equations for this motion (in rationalized m.k.s. units) are:

Maxwell's Equations/...

Maxwell's Equations

$$\text{curl } E = -\dot{B} = -\mu_o \dot{H} \tag{5.1}$$

$$\text{curl } H = \dot{D} + J = \varepsilon_o \dot{E} + N e \dot{R} \tag{5.2}$$

$$\text{div } E = \rho / \varepsilon_o \tag{5.3}$$

where the current density $J = N e \dot{R}$ (5.4)

The equation of continuity $N e \, \text{div } \dot{R} + \dot{\rho} = 0$ (5.5)

The equation of motion of electrons $e E = m \ddot{R}$ (5.6)

E, H, D, B are the well known electromagnetic field vectors.
R is a position vector in the medium.
N is the electron density.
e and m are the charge and mass of an electron respectively.

Differentiating (5.5)

$$\text{div } \ddot{R} = - \ddot{\rho} / N e \tag{5.7}$$

Taking the divergence of (5.6)

$$\text{div } \ddot{R} = e \, \text{div } E / m$$

Hence from (5.3)

$$\text{div } \ddot{R} = e \rho / m \varepsilon_o \tag{5.8}$$

Equating (5.7) and (5.8)

$$\ddot{\rho} + (N e^2 / m \varepsilon_o) \rho = 0 \tag{5.9}$$

This equation represents a simple harmonic oscillation of space charge, from which the "plasma frequency" f_o is given as

$$f_o = (N e^2 / 4\pi^2 \, m \varepsilon_o)^{\frac{1}{2}} \tag{5.10}$$

Finally the S magnetohydrodynamic wave is a longitudinal, or compression wave. At frequencies well below the ion gyro-frequency it has the velocity of sound, and when propagated along the magnetic field is almost a pure sound wave.

All four of these waves have been suggested as the cause of intense solar radio emission, but most investigators are of

the opinion /.....

the opinion that the P wave, or plasma oscillations, provides the primary mechanism. e.g. Shklovsky (1946), Bohm and Gross (1949b), Bailey (1951), Piddington (1955), Son (1955). The following objections have been raised against the plasma oscillation theory - Ryle (1949), Twiss (1951) -

(1) A plasma oscillation is essentially a longitudinal oscillation which cannot generate electromagnetic energy.

(2) Even if electromagnetic energy could be generated by plasma oscillations, the radiation could not escape because it occurs in a medium of zero refractive index.

However, Owren (1954) has demonstrated that these objections are not necessarily valid when the conditions existing in the solar athosphere are considered.

The first objection is based upon the fact that in a linear theory of small amplitude oscillations the electromagnetic field comes out as irrotational. This is a consequence of Maxwell's field equations and "Ohms Law"

$$E = \sigma J \qquad (5.11)$$

where σ is the conductivity of the medium.

From (5.4)

$$E = \dot{\sigma} N \circ \dot{R} \qquad (5.12)$$

$$\therefore \text{curl} E = \sigma N \circ \partial/\partial t \ \text{curl} R \qquad (5.13)$$

Elementary vector theory shows that

$$\text{curl} R = 0$$

$$\therefore \underline{\text{curl} E = 0} \qquad (5.14)$$

Also, from (5.1)

$$\text{curl curl} E = -\mu_0 \partial/\partial t \ \text{curl} H = 0$$

Thus

$$\underline{\text{curl} H = \dot{D} + J = 0} \qquad (5.15)$$

and the displacement current and conduction current exactly balance one another. Inclusion of a collision damping term cannot

lead to /.....

lead to electromagnetic radiation because the balance and irrotational nature of the field is preserved. Therefore, in the case of a linear small amplitude theory for a homogeneous medium with no external magnetic field, a coupling of the P mode of oscillation to the O and E modes is required for radiation of electromagnetic energy to occur.

In a non-linear theory, however, the exact balance between displacement and conduction current could be upset, and electromagnetic energy be radiated. This non-linearity is introduced if N and σ are not constant, corresponding to oscillations of large amplitude, or if a magnetic field is present in the medium. N and σ not constant would result in the following modification of (5.13)

$$\text{curl } E = e \text{ curl } \sigma N \dot{R}$$

and curl E would not in general be zero. Similarly an external magnetic field would introduce a term in $\dot{R} \times H$ in (5.12) and again curl E would not be zero. In the non-linear case radiation would be expected at harmonic frequencies.

The second objection is only appropriate if radiation is emitted at a single frequency f_0 given by (5.10). In the case of steady state oscillations, thermal motions of electrons in the plasma cause radiation to occur not just at the exact plasma frequency, but over a band of frequencies extending to both sides of it. In the transient case, investigated by Jaeger and Westfold (1949), a band of frequencies extending well above f_0 is excited, and in each of these cases frequencies greater than f_0 should be able to escape.

Having given arguments to show that plasma oscillations are capable of giving rise to electromagnetic radiation, and that this radiation can escape from the solar atmosphere, it is appropriate to discuss the excitation and decay of these oscillations. A useful analogy is to regard a plasma as a tuned circuit. Under normal conditions no oscillations occur. Two types of excitation

may be/.....

may be visualized.

(1) A positive feedback mechanism is present, so that oscillations once started grow in amplitude.

(2) An impulsive excitation is applied.

The first case has been investigated by Bohm and Gross (1949a, 1949b, 1950), who find that if a particle beam of fairly well defined velocity is injected into a main plasma with a continuous and approximately Maxwellian velocity distribution, under favourable conditions oscillations, once started, will grow in amplitude until limited by non-linear effects. The physical mechanism envisaged is one in which a group of particles, with a velocity near, but greater than the plasma wave velocity, interact strongly with the wave and transfer their kinetic energy to it. The plasma oscillations "grow" at the expense of the kinetic energy of the particles, and this growth is considerably enhanced if the plasma is of slowly varying density and the wave is moving in the direction of decreasing density.

The other case has been considered by Jaeger and Westfold (1949) who have given exact solutions for transients in an ionised medium for several specified types of initial disturbance of an electric kind. Westfold (1957) has pointed that a stream of particles injected into a compressible medium such as the solar corona is, in general, preceded by a shock wave. Across the shock front there is an abrupt transition or "jump" in the physical quantities of the medium (e.g. density, pressure, electric field etc.) which could provide the impulsive excitation envisaged.

In both of the cases considered above, when the exciting disturbance is removed, decay of the oscillations is caused by electron-electron and electron-ion collisions, the latter having a much greater effect.

The physical conditions pertaining at the time of Type II and Type III bursts point rather directly to a mechanism based

on plasma oscillations/....

on plasma oscillations. Type II bursts are known to be associated with the auroral particle streams, and Type III bursts are thought to be caused by solar "cosmic ray" particles, and these particle streams, or associated shock waves, could cause either growth or impulsive excitation of plasma oscillations in localized regions of the solar atmosphere. The observed characteristics of Type III bursts listed at the beginning of this chapter are all consistent with this idea. However, attempts to account quantitatively for the detailed characteristics of isolated bursts in terms of plasma oscillations are frustrating because so little is known of the initiating disturbances and of the electron density, electron temperature, magnetic field conditions and other relevant parameters applicable to the solar atmosphere under disturbed conditions. In practice attention must be confined to simple idealized cases, two of which are described below.

(1) Jaeger and Westfold (1949)

These writers investigated theoretically transient radio emission from a stationary, localized source in the solar atmosphere. They specified several initial disturbances of an electric type, corresponding to jumps in electric field and polarization both at a plane and over a finite region in the plasma. In practically all cases the transient response of the medium shows a sharp maximum in intensity at the plasma frequency f_o , a sharp cut-off below f_o , and a gradual decrease with increasing frequency for frequencies greater than f_o . A typical spectrum of a transient is shown below.

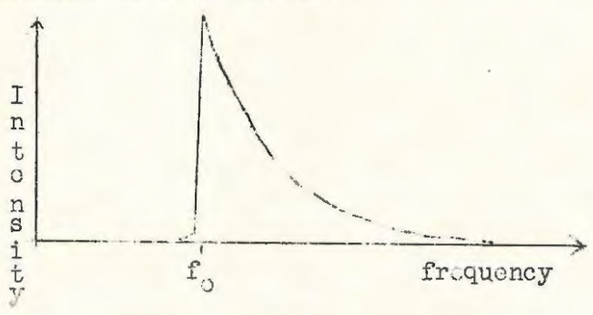

For a stationary source at the plasma level f_o they expected the dynamic spectra of isolated bursts to show the

following characteristics/.

following characteristics:

(1) Radiation would be emitted on all frequencies greater than f_o , and there would be no emission on frequencies less than f_o.

(2) The peak intensity would show a rapid frequency drift in the direction of decreasing frequency caused by selective group retardation.

(3) The peak intensity would be a maximum at f_o and decrease for higher values of frequency according to a law such as f^{-2} or f^{-4} ; the expected variation of peak intensity with frequency is shown in the above diagram.

(4) The intensity at any particular frequency f would decay with time, possibly with a time factor $\exp (-\nu t)$ where ν is the effective collision frequency for the frequency considered at the f_o level.

(5) Echoes, caused by reflection of frequencies greater than f_o from their respective plasma levels would be expected. The echo would be of lower intensity than the direct wave, and would arrive later. Figure 2:1 illustrates typical trajectories for the direct and echo wave.

These predictions were compared with Payne-Scott's (1949) single frequency observations, and the qualitative agreement was found to be good. The observed double-humped bursts were interpreted as echoes. However, interpretation of the dynamic spectra of isolated bursts by Wild (1950b) showed that his double-humps did not have the spectra expected on the echo hypothesis. Furthermore, he showed that the observed frequency drift of Type III bursts could not be accounted for by group retardation alone, irrespective of assumptions concerning coronal electron density distribution.

(2) Wild (1950b) Pawsey and Smerd (1953)

(a) The frequency drifts of Type III bursts are interpreted in terms of the outward motion of localized disturbances in the solar atmosphere. The mechanism depends on two ideas:

(1)/.....

(1) Emission of coherent radiation in the solar atmosphere occurs in a band of frequencies near the plasma frequency f_o at which the refractive index is zero.

(2) The value of f_o in the solar atmosphere decreases with height. This follows from equation (5.10) if N is assumed to decrease continuously with height.

As has been mentioned previously, source velocities derived on this hypothesis are about one tenth of the velocity of light in free space.

(b) Decay at each frequency is attributed to the natural decay of plasma oscillations, in which case the exciting source can persist at a given level only during the period of growth of the burst. For this hypothesis to hold, oscillations from a particular level must be emitted in a narrow frequency band , to permit the exciting agency to move outside this band in a time small compared with the decay time of the burst. The observed exponential decay constant at any particular frequency may be identified with the collision frequency near the level of zero refractive index for the frequency considered. On the usual assumptions regarding coronal electron temperature and density, the collision frequency decreases continuously with height -- see for instance Table 2/1 -- and hence the observed decrease in decay constant with decreasing frequency is taken to be further evidence in favour of the outward moving agency hypothesis. On this theory, the bandwidth and instantaneous shape of frequency profiles are regarded as dependent properties determined by the drift rate and lifetimes measured over a sufficiently broad frequency range.

This interpretation is discussed further in Chapter Seven with reference to the author's and other observations.

TABLE 6/1

OBSERVATIONS OF SINGLE PEAKED ISOLATED BURSTS ON 125 MC./S.

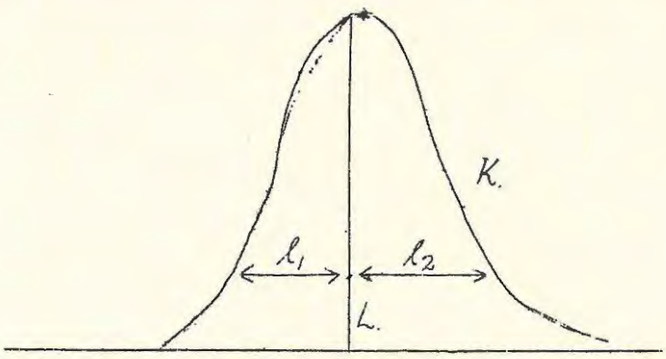

Record No.	Date.	Time U.T.	Decay constant k sec.$^{-1}$	l_1 secs.	l_2 secs.	Lifetime L secs.
A 53	18/12/57	11:40	0.286	2.60	4.71	7.31
A 53	18/12/57	14:55	*	1.24	0.79	2.03
A 55	20/12/57	10:31	0.504	1.39	3.15	4.54
A 57	22/12/57	08:54	1.865	0.99	0.77	1.76
A 58	23/12/57	14:40	0.686	1.36	1.64	3.00
A 69	13/ 1/58	10:16	0.607	1.36	2.88	4.24
A 69	13/ 1/58	10:34	0.480	2.55	3.62	6.17
A 69	13/ 1/58	12:27	1.390	2.11	1.11	3.22
A 70	14/ 1/58	13:21	0.917	1.07	0.77	1.84
A 71	15/ 1/58	07:33	0.571	1.51	2.55	4.06
A 72	16/ 1/58	12:19	1.180	1.29	1.66	2.95
A 72	16/ 1/58	12:27	0.647	1.49	2.48	3.97
A 72	16/ 1/58	12:58	1.075	-	-	-
A 79	24/ 1/58	07:34	0.522	2.33	2.33	5.16
A 83	29/ 1/58	10:47	0.912	1.61	0.99	2.60
A 87	3/ 2/58	07:23	0.410	2.73	1.24	3.97
A 87	3/ 2/58	10:18	0.523	3.10	2.85	5.95
A 89	6/ 2/58	10:37	1.350	1.14	1.29	2.43
AVERAGE VALUES			0.819	1.79	2.05	3.84

* The tail portion of this burst was definitely not exponential. In this case the "rise" portion of the burst profile appeared to be exponential, which seems to indicate that this is a reversed burst.

TABLE 6/2.

LIFETIMES OF DOUBLE-HUMPED ISOLATED BURSTS ON 125 MC./S.

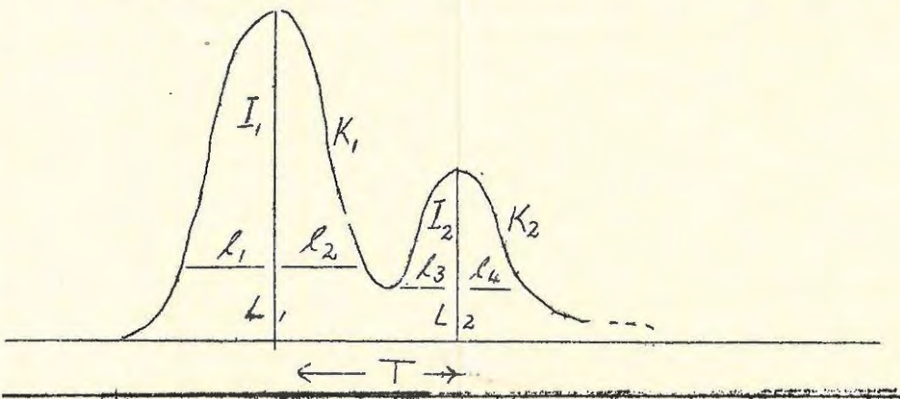

Record No.	Date	Time U.T.	l_1 secs.	l_2 secs.	Life-time L_1 secs.	l_3 secs.	l_4 secs.	Life-time L_2 secs.
A 37	28/11/57	10:34	1.04	2.18	3.22	2.23	4.34	6.57
A 45	7/12/57	13:12	4.96	6.50	11.46	2.60	2.11	4.71
A 50	13/12/57	07:46	3.10	-	-	-	2.48	-
A 50	13/12/57	10:58	-	-	-	-	2.11	-
A 50	13/12/57	12:18	-	-	-	-	2.36	-
A 52	17/12/57	12:52	1.98	1.79	3.77	-	3.72	-
A 55	20/12/57	09:18	2.23	1.86	4.09	2.93	5.75	8.68
A 58	23/12/57	14:41	1.26	2.78	4.04	1.66	3.42	5.08
A 69	13/ 1/58	12:03	2.60	3.27	5.87	4.89	4.04	8.93
A 71	15/ 1/58	07:35	0.74	-	-	-	1.69	-
A 78	23/ 1/58	09:12	2.98	3.22	6.20	-	2.48	-
A 79	24/ 1/58	11:30	2.11	-	-	-	2.98	-
A 87	3/ 2/58	07:20	2.41	-	-	-	1.86	-
A 87	3/ 2/58	14:37	1.98	1.74	3.72	-	3.10	-
AVERAGE VALUES			2.28	2.92	5.30	2.86	3.03	6.79

N.B. Blanks appear in the above table where it was not possible to measure the lifetimes.

TABLE 6/3.

OBSERVATIONS OF DOUBLE-HUMPED ISOLATED BURSTS ON 125 MC./S.

Record No.	Date.	Time U.T.	k_1 sec^{-1}	k_2 sec^{-1}	I_1/I_2	T secs.	Velocity V in units of 104 km./sec.
A 37	28/11/57	10:34	0.428	0.599	2.26	8.70	1.33
A 45	7/12/57	13:12	0.273	0.871	1.78	18.40	0.64
A 50	13/12/57	07:46	0.238	0.650	1.24	3.60	3.02
A 50	13/12/57	10:44	-	-	1.55	10.50	1.11
A 50	13/12/57	10:58	0.427	0.695	1.74	4.83	2.31
A 50	13/12/57	12:18	0.647	0.685	2.21	4.51	2.46
A 50	13/12/57	12:32	0.824	0.571	1.58	4.14	2.67
A 52	17/12/57	11:26	-	-	0.81	5.60	2.02
A 52	17/12/57	12:52	0.667	0.476	3.02	5.81	1.95
A 55	20/12/57	09:18	0.915	0.320	2.50	14.40	0.82
A 55	20/12/57	13:43	-	-	1.76	5.34	2.11
A 58	23/12/57	14:41	0.561	0.508	2.08	7.19	1.59
A 63	6/ 1/58	12:53	-	-	3.82	11.80	0.99
A 69	13/ 1/58	10:48	-	-	1.73	9.60	1.21
A 69	13/ 1/58	12:03	0.475	0.360	1.51	12.40	0.94
A 71	15/ 1/58	07:35	1.180	0.990	1.35	2.54	4.12
A 78	23/ 1/58	09:12	0.570	0.695	2.67	7.62	1.51
A 78	23/ 1/58	09:26	-	-	0.40	5.66	2.00
A 79	24/ 1/58	11:30	0.361	0.495	1.43	3.39	3.20
A 87	3/ 2/58	07:20	0.404	0.837	1.76	4.20	2.63
A 87	3/ 2/58	14:37	0.990	0.456	2.68	5.11	2.20
AVERAGE VALUES			0.597	0.614	1.90	7.40	1.94

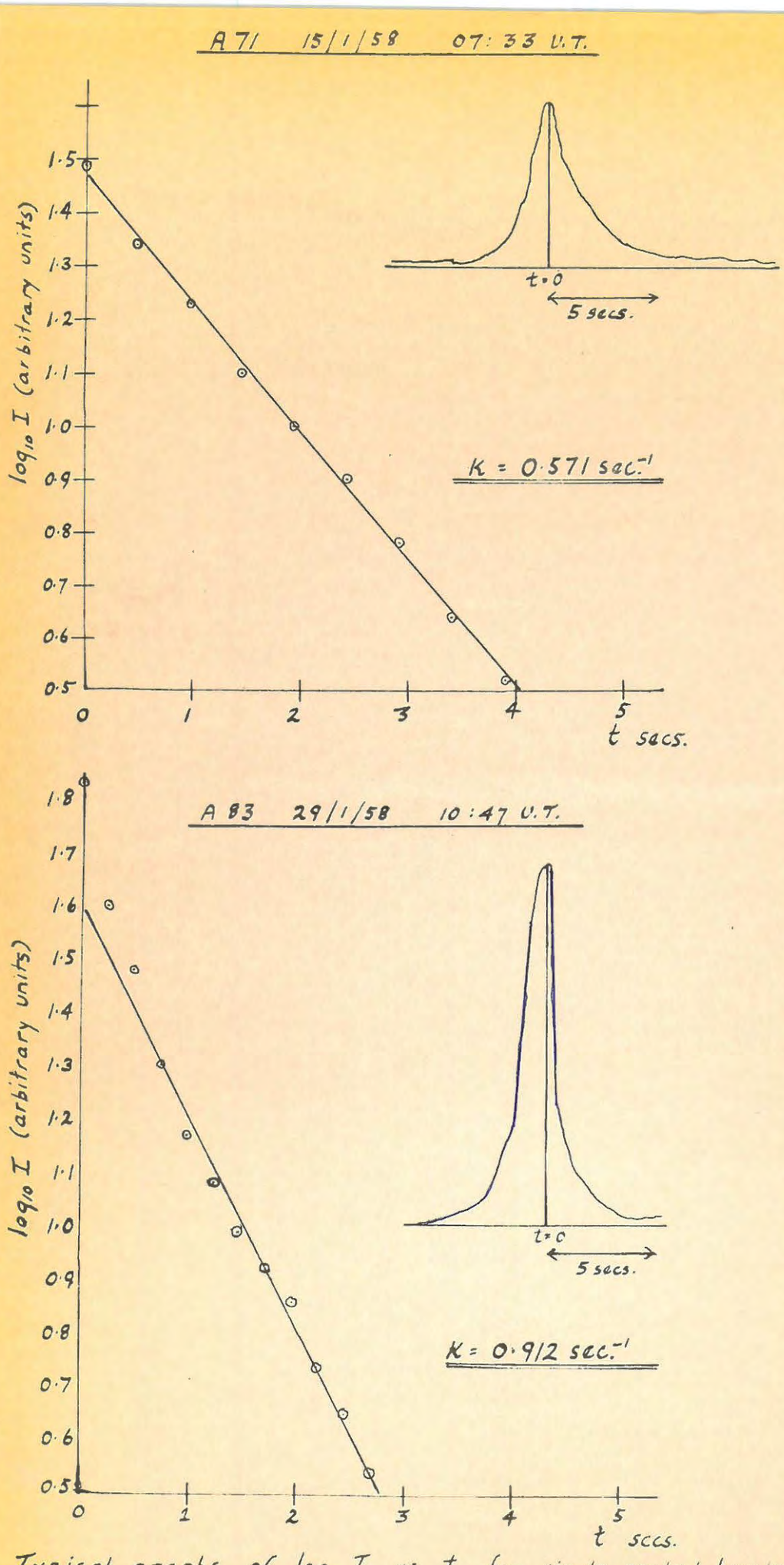

Typical graphs of $\log_{10} I$ vs t for single peaked bursts.

FIGURE 6:1

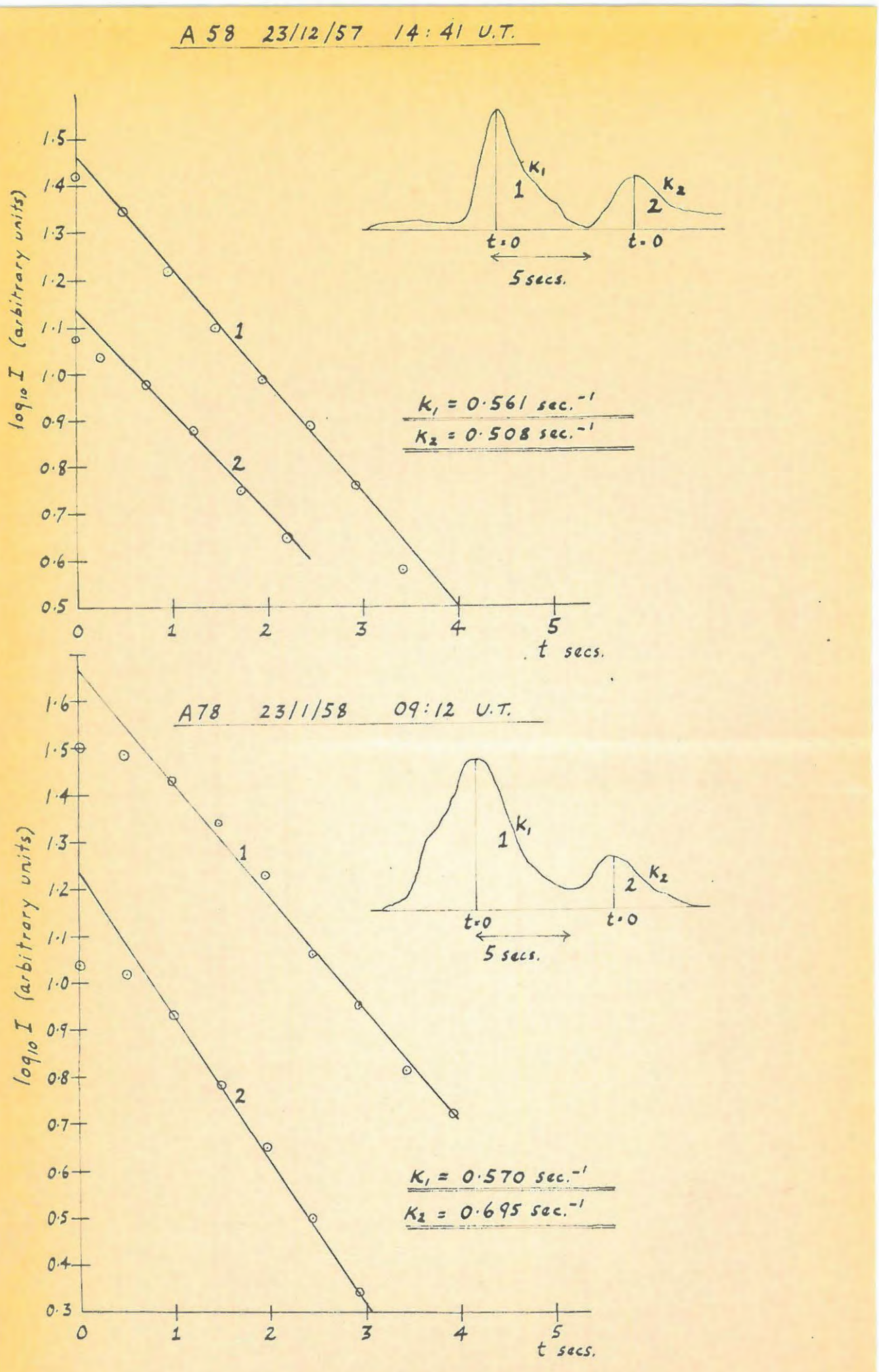

Typical graphs of $\log_{10} I$ vs t for double-humped bursts.

FIGURE 6:2

CHAPTER SIX

OBSERVATIONS OF ISOLATED BURSTS ON 125 MC./S.

Film records representing approximately 375 hours of solar radio noise observations taken during the period November 26 · 1957 — February 6 1958 were examined by the author. Only isolated bursts having a single peak and double-humped bursts were selected for analysis, and during the period mentioned 13 of the former and 21 of the latter were found to be sufficiently well defined for analysis - typical burst profiles are shown in Plate D. These selected bursts were true isolated bursts in the sense that they occurred isolated from noise storms. Burst profiles were analysed, after projecting the film records, with a magnification of about 16 X , onto graph paper, and drawing the centre line of the photographic trace of the cathode ray tube spot.

In the case of bursts having a single peak, the lifetime L (measured between points of $\frac{1}{e}$ maximum intensity) was determined for each burst. A graph of $\log_{10} I$ versus t (where I is intensity and t time) was plotted for the tail portion of every burst. The base level of intensity (i.e. I = 0) was taken as the level · before the burst appeared, and t was arbitrarily assigned to be zero at the peak of the burst. These graphs were good approximations to straight lines in nearly all cases, verifying that burst tails are approximately exponential in shape, and the exponential decay constant k was found from the slope of the graph in each case — typical graphs are shown in figure 6:1. A summary of the results obtained for single peaked bursts is given in Table 6/1.

Lifetimes of both the first and second peaks of double-humped bursts (L_1 and L_2) were measured where possible, and exponential decay constants for each hump (k_1 and k_2) were derived in the manner outlined above — typical graphs are shown in figure 6:2. In addition, the time difference T between the peaks, and the ratio of peak intensities I_1 / I_2 was measured in each case. The results obtained are summarized in Tables 6/2 and 6/3.

SUMMARY/.....

SUMMARY OF RESULTS

The general features of isolated burst profiles recorded were found to be consistent with those reported by other observers. Comparisons are given below:

(1) Lifetimes

L_{av} = 3.8 secs. — 53% of the lifetime spent in decay

$L_{1\,av}$ = 5.3 secs. — 56% "

$L_{2\,av}$ = 6.8 secs. — 51% "

cf. Wild (1950b) — 100 Mc./s. — $2.9 < L$ (secs.) < 3.8 — about 60% of the lifetime spent in decay.

(2) Decay Constants

k_{av} = 0.52 $sec.^{-1}$

$k_{1\,av}$ = 0.60 "

$k_{2\,av}$ = 0.61 "

cf. Williams (1948) — 75 Mc./s. — k_{av} = 0.7 $sec.^{-1}$

Payne-Scott (1949) — 85 " — " = 0.6 "

60 " " = 0.6 "

19 " " = 0.2_5 "

Wild (1950b) — 100 " — " = 1.0 "

(3) Peak Intensity Ratios of Double-Humped Bursts

$I_1 / I_{2\,av}$ = 1.9

cf. Payne-Scott (1949) — 85 Mc./s. — $I_1 / I_{2\,av}$ = 4

60 Mc./s. " = 4

(4) Time Delays Between Peaks of Double-Humped Bursts

T_{av} = 7.4 secs.

cf. Payne-Scott (1949) — 35 & 60 Mc./s. $2 < T$ (secs.) < 10

* * * * *

ACKNOWLEDGEMENT

Throughout the period November 26 1957 — February 6 1958 the equipment was operated, and the film records were developed by Mr. R.G.Speedy. However, during November the author spent about 30 hours operating the equipment and monitoring the received signals, and became thoroughly familiar with the operating procedure. Further, Dr. Stack-Forsyth, the author, and Mr. Speedy spent many happy hours attempting to persuade electronic voltage regulators to regulate, and R.F. amplifiers to desist from oscillating, during which some knowledge was gained of the vagaries to which electronic equipment is subject.

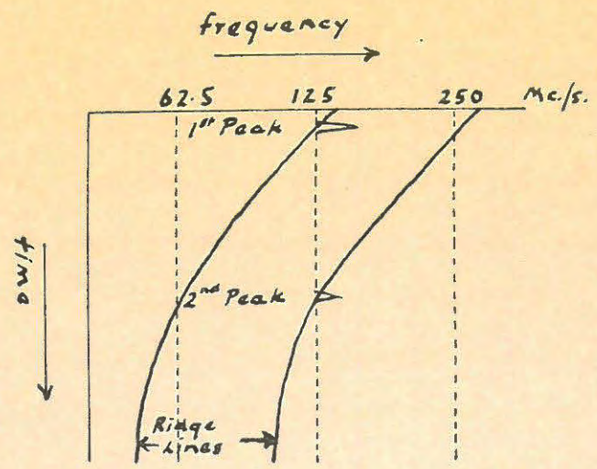

A hypothetical dynamic spectrum to explain double-humped bursts on 125 Mc./s.

FIGURE 7:1

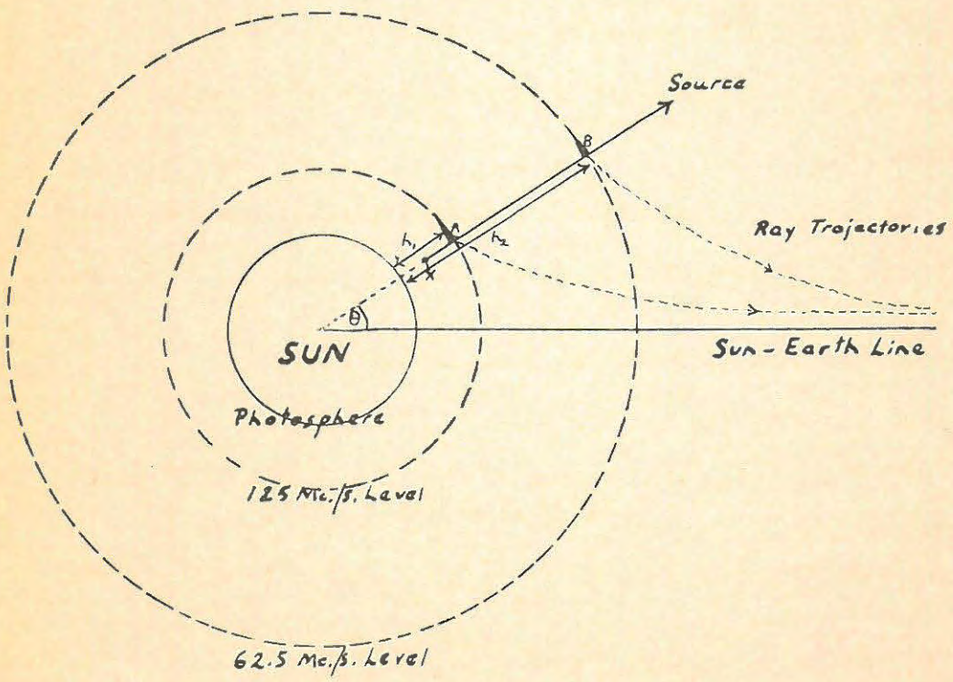

Formation of Double-Humped Bursts in the Solar Atmosphere

FIGURE 7:2

CHAPTER SEVEN

INTERPRETATION OF OBSERVATIONS

A: Double-Humped Bursts

The author suggests that the first peak of his observed double-humped bursts originates at the level of zero refractive index for 125 Mc./s. radiation, and that the second peak is the second harmonic of 62.5 Mc./s., and consequently originates at the 62.5 Mc./s. level. On this hypothesis the observed time delay T between the peaks is attributed to the time of travel of an outward moving source between the 125 and 62.5 Mc./s. levels. A hypothetical dynamic spectrum illustrating the manner in which double-humped bursts arise is shown in figure 7:1. Source velocities may be calculated if some assumptions are made: viz,

(1) The source moves radially outwards.

(2) The source travels with constant velocity.

(3) The first and second peaks are associated with the 125 and 62.5 Mc./s. levels respectively.

(4) The Baumbach-Allen coronal electron distribution is assumed.

An example illustrating how source velocities may be calculated from the values of T is given below:

A typical time delay between the peaks is 6.0 secs.

Referring to figure 7:2

h_2 = height above the photosphere of the 62.5 Mc./s. level = 17.5×10^4 km.

h_1 = height above the photosphere of the 125 Mc./s. level = 5.4×10^4 km.

$\therefore$ Distance AB = $h_2 - h_1 = 12.1 \times 10^4$ km.

(These values of h have been derived from the Baumbach-Allen formula, and are listed in Table 2/1)

Now consider a source travelling radially outwards from its origin at X. When it reaches A, 125 Mc./s. radiation corresponding to the first peak is emitted. Neglecting the effect of

group retardation/.....

group retardation and for a source angle $\theta = 0$, the electromagnetic radiation takes about

$$\frac{h_2 - h_1}{c} = \frac{12.1 \times 10^4 \text{ km.}}{3.0 \times 10^5 \text{ km./sec.}} = 0.4 \text{ seconds}$$

to reach B. If the source takes 6.4 seconds to reach B and excite radiation corresponding to the second peak, the time difference between the peaks at B would be 6.0 seconds. From the point B to earth radiation corresponding to the first and second peaks travels at the same velocity, and hence the observed time delay between the peaks at earth is about 6.0 seconds. Thus, to obtain the time of travel of the source between the 125 and 62.5 Mc./s. levels, it is necessary to add a small correction amounting to about 0.4 seconds to the observed time delay T between the peaks.

The source velocity V may now be calculated:

$$V = \frac{AB \text{ km.}}{(T + 0.4) \text{ secs.}}$$

$$= \frac{12.1 \times 10^4}{6.4} \text{ km./sec.}$$

$$= 1.9 \times 10^4 \text{ km./sec.}$$

The time delays T for 21 observed double-humped bursts varied between 2 and 18 seconds, and source velocities calculated in the manner outlined above were in the range $0.6 - 4.1 \times 10^4$ km./sec., with an average value of 1.9×10^4 km./sec. Values of V for individual bursts are listed in Table 6/3. These values are in good agreement with those obtained by the author from Payne-Scott's (1949) observations of the time delays between corresponding bursts on different frequencies, and those derived by Wild (1950b) from the drift rates of Type III bursts - see Chapter Four - and hence it seems very likely that this interpretation of double-humped bursts is correct.

B: Exponential Decay Constants

On the assumption that the model of Wild (1950b) and

Pawsey and Smerd/.....

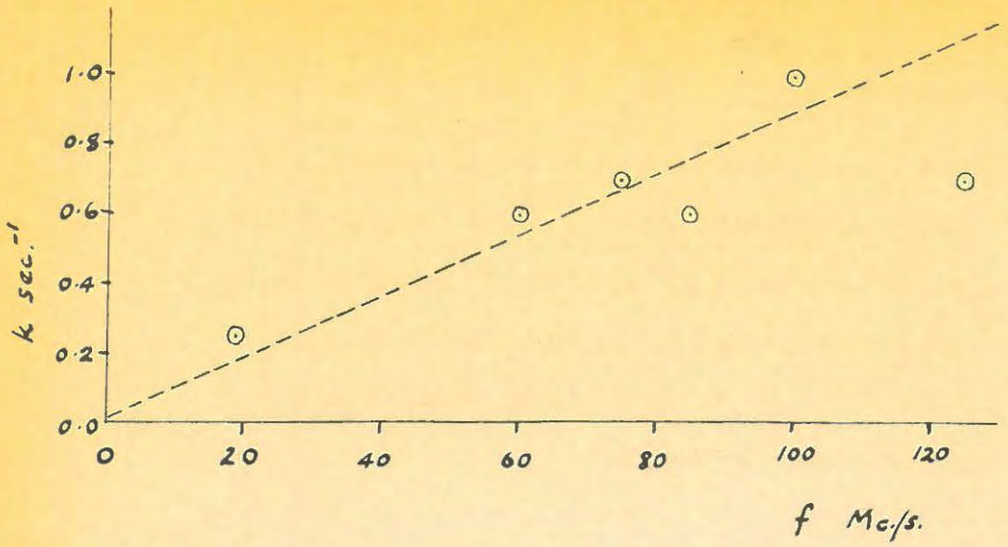

Observed values of the exponential decay constant k of isolated bursts.

FIGURE 7:3

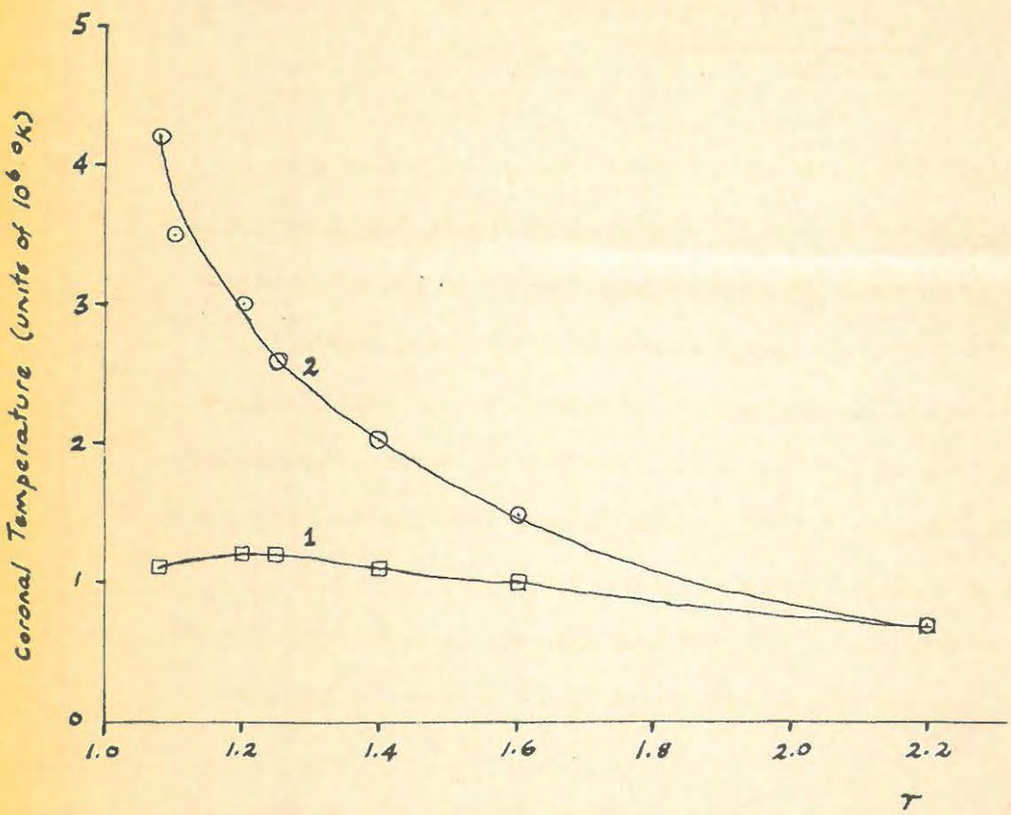

r = height in the solar atmosphere in units of 1 solar radius

Plot of Coronal Temperature vs Height in the Solar Atmosphere

Curve 1 shows temperatures derived from equation (2.2)

Curve 2 shows temperatures derived from decay constants of isolated bursts.

FIGURE 7:4

Pawsey and Smerd (1953) given in Chapter Five is correct, the exponential decay constant k of isolated bursts at a particular frequency f_o may be equated to the collision frequency ν at the f_o level of zero refractive index. The collision frequency is given approximately in terms of the electron density N and the electron temperature T by the formula

$$\nu = 42 \, N \, T^{-3/2} \qquad \text{see equation} \quad (2.5)$$

and f_o is given in terms by equation (2.3). Hence the measured values of f_o and k enable the kinetic temperature T to be estimated from the formula

$$T = \left\{ \frac{5.2 \times 10^{-7} \; f_o^{\,2}}{k} \right\}^{2/3}$$

Figure 7:3 shows the observed average values of k on frequencies between 19 and 125 Mc./s., and figure 7:4 shows the variation of electron temperature with height in the solar atmosphere derived from the decay constants of isolated bursts and from equation (2.2). Observations of the width of coronal emission lines by Waldmeier (1947) suggest that the coronal temperature distribution is similar to that deduced from the decay constants of isolated bursts.

However, recent observations have cast considerable doubt upon this interpretation. Some criticisms which may be levelled at it are:

(1) Pawsey and Smerd (1953) have pointed out that if the decay of isolated bursts observed on any frequency f_o is a representation of the natural decay of plasma oscillations, frequencies must be excited in a narrow band about the plasma frequency f_o. In this case escape of radiation would be possible for source angles θ near zero. The results of Loughhead et al (1957) show that Type III events are approximately uniformly distributed across the solar disk, implying that escape of radiation is possible for large source angles.

(2)/.....

A 53 18/12/57 14 : 55 U.T.

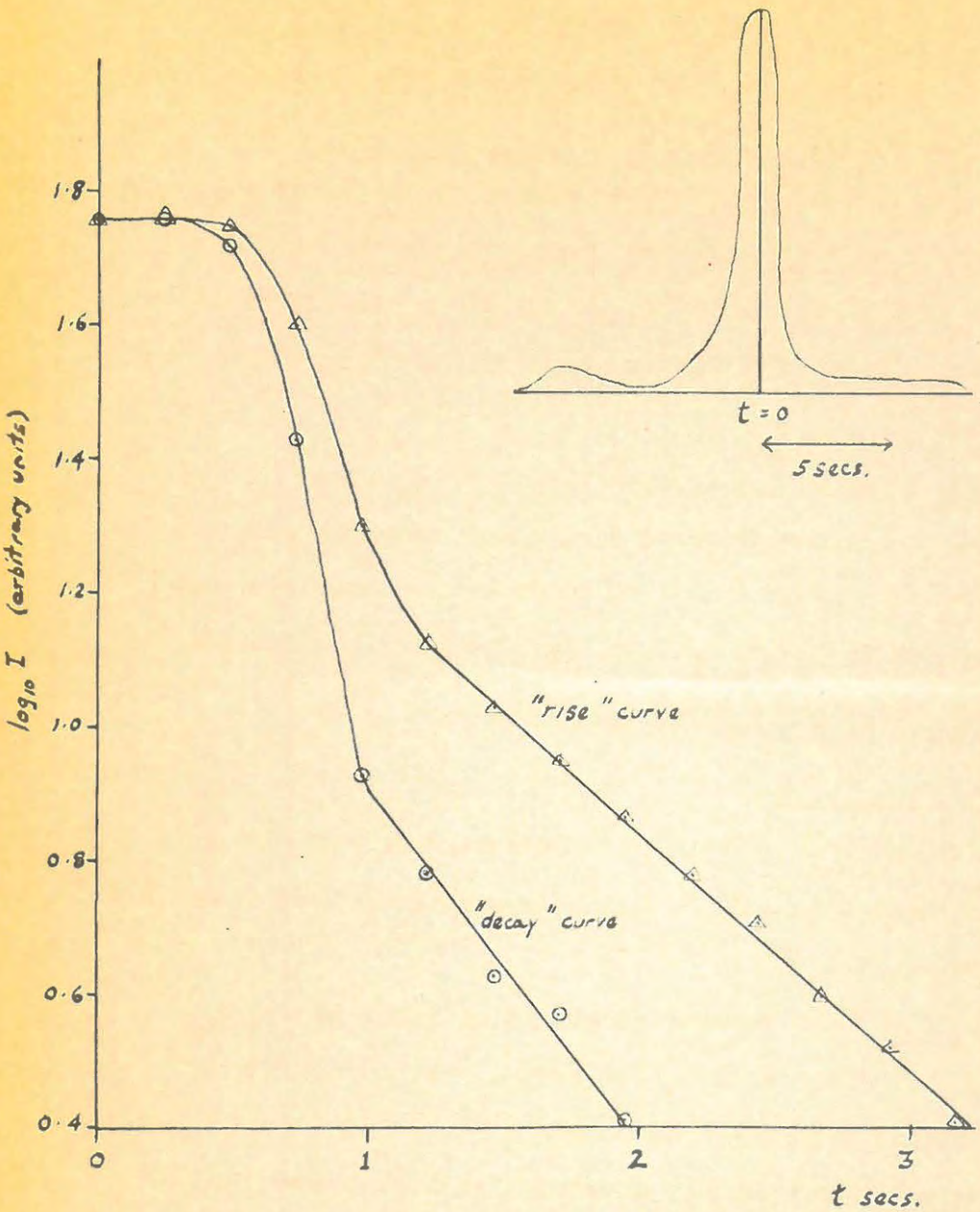

A reversed single peak burst.

N.B. The time scale for the "rise" curve has been reversed in plotting the above graph.

FIGURE 7:5

(2) Single peaked bursts, and the first peak of double-humped bursts on the same frequency are believed to originate at the same level in the solar atmosphere, and consequently the decay constants of each are expected, on the average, to be equal. However, both Payne-Scott (1949) and the author have found that single peaks tend to decay more rapidly than the first peak of double-humped bursts.

(3) A few bursts have been observed in which the rise profile has the shape of a reversed exponential curve, whereas the decay profile is definitely not exponential. An example is shown in figure 7:5. On the above theory it is not possible to account for this phenomenon.

These inconsistencies, in particular the fact that radiation emitted in a narrow frequency band cannot escape for even moderate source angles, led the author to suggest an alternative model. Before this is discussed, the nature of the exciting disturbances will be reviewed briefly.

C: Exciting Disturbances

In considering generation of electromagnetic radiation in the solar corona by travelling disturbances, four distinct cases may be envisaged:

(1) A localized source causing emission of radiation in a narrow frequency band in the region of the source. This corresponds to the case which has just been discussed.

(2) An extended source causing emission of radiation over a large range of plasma levels simultaneously, the emission at any particular level occurring in a narrow band.

(3) A localized source causing emission of radiation in a broad frequency band in the region of the source.

(4) An extended source emitting radiation over a large range of plasma levels simultaneously, the emission at any particular level occurring in a broad band.

Cases (1) and (2) above are open to the same criticism;

namely/.....

namely, if radiation is emitted in a narrow frequency band in a region where the refractive index is zero, escape is only possible for small source angles, which is not in agreement with the results of Loughhead et al. However, in cases (3) and (4) escape is in general possible. If reversed double-humped bursts are interpreted as emission by sources moving inwards and exciting first the second harmonic at the 62.5 Mc./s. level, and then the fundamental at the 125 Mc./s. level, case (4) may be ruled out. The argument, with reference to Plate D (6), is as follows:

The second peak of the reversed burst shown is very much sharper and has a shorter lifetime than the first peak. If these bursts were produced by an extended source moving outwards, a sharp first peak and more extended second peak, resulting from velocity spread in the source, would be expected. This argument is admittedly based on insufficient observational evidence, but nevertheless only case (3) will be considered in formulating an alternative model for isolated bursts.

D: The Author's Model

An outward moving localized source giving rise to emission of radiation in a broad frequency band is considered. Jaeger and Westfold (1949) state that, for a localized instantaneous disturbance at the f_o plasma level, the spectrum of the generated radiation has the following characteristics:

(1) Radiation is emitted on all frequencies above f_o, and there is no radiation on frequencies less than f_o.

(2) The intensity at high frequencies falls of as f^{-n}, where n is either 2 or 4.

(3) Intensity decays with time like $\exp(-\nu t)$.

The generated profile of a Jaeger-Westfold transient is shown below:

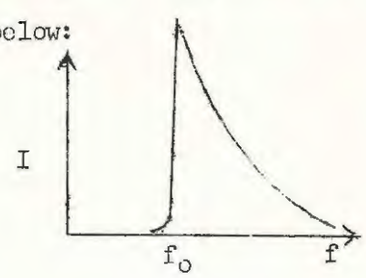

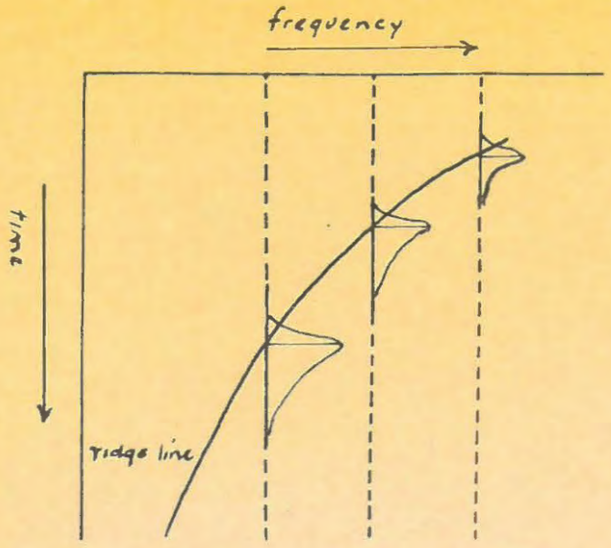

(a) Dynamic Spectrum of a Type III event according to Wild (1950b), Pawsey and Smerd (1953)

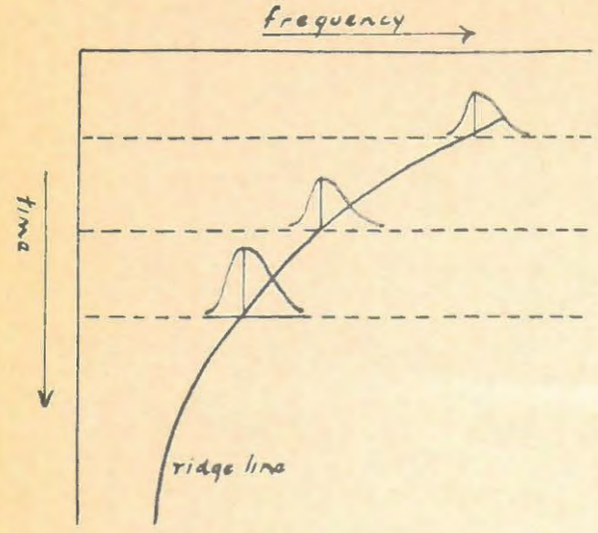

(b) Dynamic Spectrum according to the author's model

FIGURE 7:6

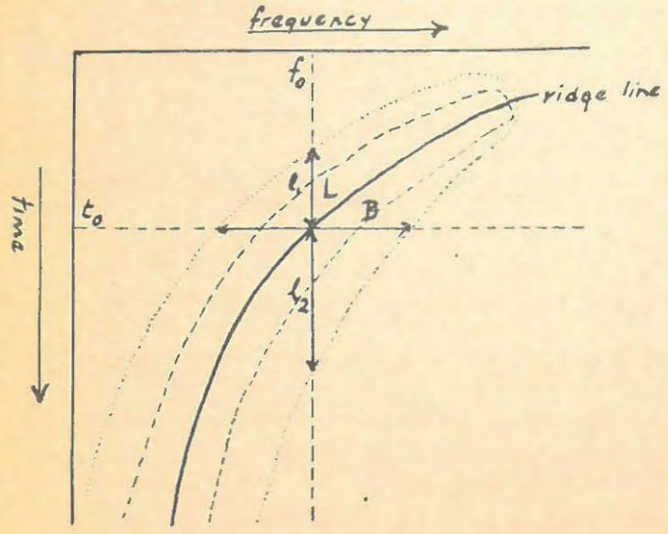

Contour Diagram of an Idealized Type III Burst.

B = Bandwidth measured between points of ¼ maximum intensity

L = Lifetime measured between points of ¼ maximum intensity

FIGURE 7:7

A disturbance moving outwards in the solar corona - i.e. to lower plasma frequency levels - produces spectra similar to that shown above, but displaced to the left along the frequency axis. If then the intensity at a single frequency is observed, the time profile is expected to vary in a similar sort of fashion as the frequency profile provided that:

(1) There is no transmission loss.

(2) The radiation decays infinitely rapidly, so that at any instant the received radiation is generated at one level in the solar atmosphere.

The generated time profile is shown in (a) below:

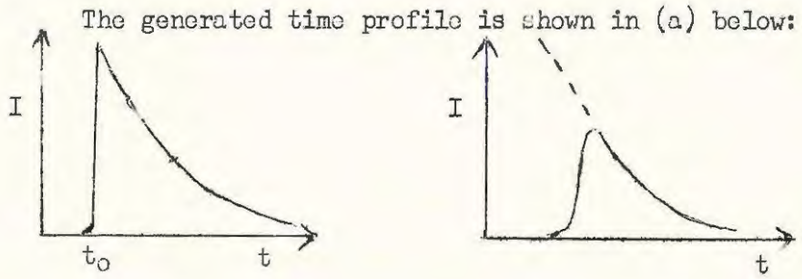

The received time profile is like (b). It differs from the generated profile on account of propagation losses along the path to the receiver.

Figure 7:6 illustrates how the dynamic spectrum of observed Type III bursts is formed according to this model. In this case radiation observed at any given time is regarded as originating at one level in the solar atmosphere. Also shown is the composition of a Type III burst according to Wild, Pawsey and Smerd, and on this model radiation observed on any given frequency is regarded as originating at one level in the solar atmosphere. Thus, according to the author's model the frequency profiles and instantaneous bandwidths are considered to be fundamental properties of a burst, whereas the time profiles, lifetimes and decay constants are dependent properties determined by the instantaneous frequency profiles, and the drift rate throughout the lifetime of the burst. This is the direct opposite of the view put forward by Wild, Pawsey and Smerd - see Chapter Five.

Reference to figure 7:7 shows that the bandwidth B at time t_o , the lifetime L on a frequency f_o , and the drift rate at (f_o , t_o) are approximately related by the following expression

$$L = \frac{B}{\left\{\frac{df}{dt}\right\}_{f_o,\, t_o}} \qquad (7.1)$$

where f_o , t_o refer to a point on the ridge line. Wild (1950b) has shown that along the ridge line

$$\frac{df}{dt} \propto f \qquad \text{see equation (4.3)}$$

and therefore

$$L \propto B/f$$

From this relation it may be seen that, if the bandwidth is a fundamental property of isolated bursts, and remains approximately constant throughout the duration of the burst, the lifetime would increase at decreasing frequencies, which is in accordance with observations. Similarly, the decay constant k which is approximately proportional to the reciprocal of the decay lifetime l_2 would be expected to decrease with frequency according to the relation

$$k = K f$$

where K is a constant.

This is precisely the relation obtained by Wild (1950b) - see equation 4:1 - and figure 7:3 offers further support for this relation. Wild's (1950b) contour diagrams of Type III bursts show that the bandwidth of any given burst does in fact remain approximately constant, with perhaps a slight tendency to increase at low frequencies. On this model the inconsistencies which were noticed in applying the model of Wild, Pawsey and Smerd may be explained.

(1) Escape of Radiation

At any given level in the corona radiation generated on frequencies below the critical escape frequency f_c is expected to be strongly attenuated. Smerd has shown that the critical escape

frequency/.....

frequency f_c is approximately related to the plasma frequency f_o at the same level in the Baumbach-Allen corona by the expression

$$f_c = f_o \sec 0.87\,\theta \qquad \text{see equation} \qquad (2.13)$$

for source angles θ between 0° and 80°, and frequencies of the order of 100 Mc./s.

The author's model provides justification for the comparison of the instantaneous frequency profiles of the fundamental and harmonic bands of Type III events, and the observed cut-off in the fundamental band supports the idea that the low frequency edge of the fundamental band is cut off during escape. The peak in intensity of the fundamental band is normally expected at a frequency slightly greater than f_c, and the peak of the harmonic band at a frequency $2f_o$. Thus, from the observations of Wild, Murray, and Rowe (1954) that the instantaneous frequency ratio of peak intensities lies between 1.85 and 2.00, the range of source angles for which escape of radiation in the fundamental band is possible may be calculated from (2.13). The result obtained is that θ varies between 0° and 35°, implying that radiation may be received from bursts occurring over practically the entire optical disk. This result is consistent with the observations of Loughhead *et al*.

(2) Lifetimes and Decay Constants

Observations by Payne-Scott (1949) and the author show that, on the average, single peaks decay more rapidly and have a shorter lifetime than the first peak of double-humped bursts. Equation (7.1) shows that an explanation for this may be that the bandwidth of single peaks is smaller, and/or the drift rate is greater. Comparison of the bandwidths and drift rates of Type III events, both with, and without a harmonic band, should settle this question.

Furthermore, on this theory the "decay" portion of burst profiles is regarded as a decrease in the influence of the excit-exciting source, rather than a natural decay of plasma oscillations and consequently burst profiles would not necessarily be

exponential/.....

A 72 16/1/58 12:27 U.T.

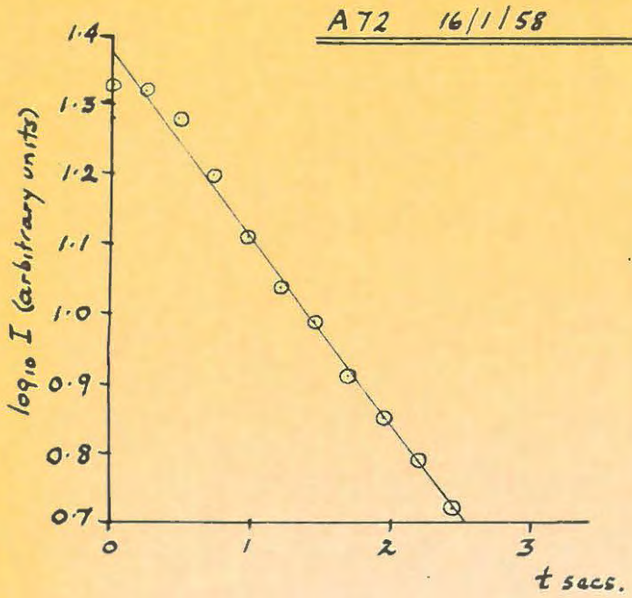

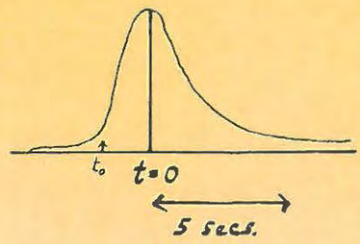

Exponential plot for the above burst.

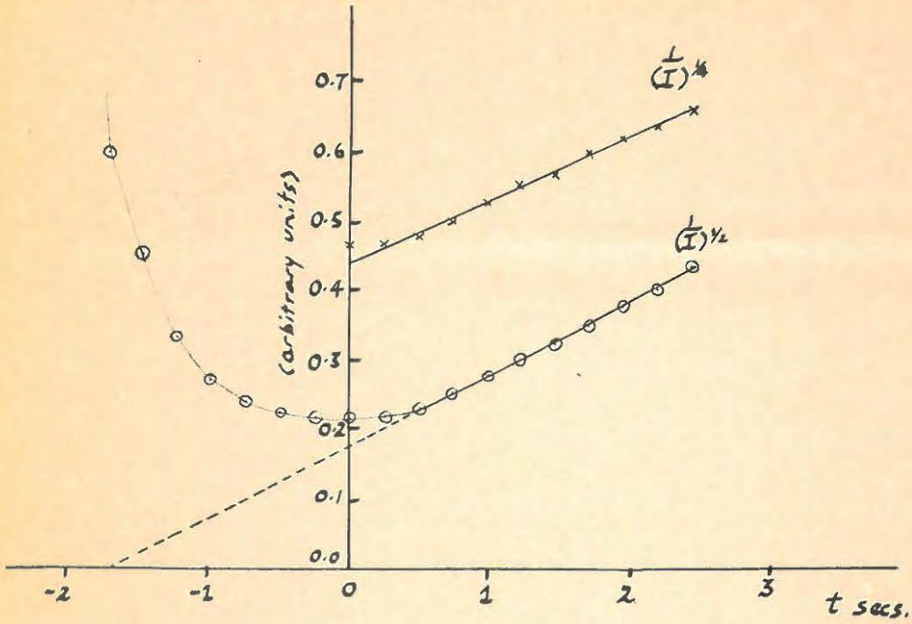

Plots of $\frac{1}{(I)^{1/4}}$ and $\frac{1}{(I)^{1/2}}$ vs t for the same burst.

FIGURE 7:8

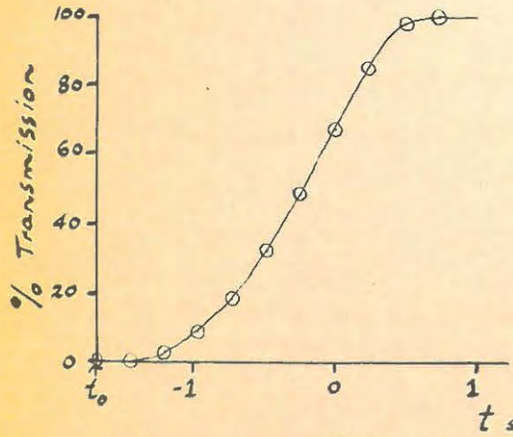

A line-of-sight transmission curve for 125 Mc./s. radiation deduced from the "rise" profile of the above burst.

FIGURE 7:9

exponential. In fact, they appear to fit a relationship of the form $I^{-1/n} \propto t$ fairly well. Figure 7:8 shows plots of $I^{-\frac{1}{2}}$ vs t and $I^{-\frac{1}{4}}$ vs t for the tail portion of a typical isolated burst. Also shown is the exponential plot of $\log_{10} I$ vs t. All 3 plots are fairly close approximations to straight lines, and it was not possible to decide, from the data available, what the value of n in the above relation was, nor whether the above relation was a better fit than the exponential function.

(3) Reversed Bursts

Bursts caused by inward moving localized disturbances would be expected, on this theory, to have profiles which are a mirror image of normal burst profiles, whereas, on the Wild, Pawsey and Smerd model, bursts would have the characteristic sharp rise and exponential decay, whether caused by outward or inward moving disturbances. Thus, this theory provides a natural explanation for reversed bursts.

(4) Propagation Losses

Two factors contribute to attenuation of radiation between the region of origin in the solar atmosphere and a terrestial observer. These are:

(i) The obliquity factor, which has been discussed in section (1) above. The effect of this is to give a sharp cut-off on all frequencies below the critical escape frequency f_c.

(ii) Absorption, which depends largely upon the collision frequency ν given by (2.5). The total absorption for radiation escaping the solar atmosphere from a height r is given by an integral of the form

$$I = I_o \, e^{-\int_r^\infty k \, ds} \qquad \text{(Jaeger and Westfold, 1950)}$$

where ds is an element of path, and

$$k = \text{the absorption coefficient} = \frac{\nu}{2c} \frac{1 - \mu^2}{\mu}$$

Radiation near the tail of a burst will be generated when the exciting source has moved some distance out from the f_o plasma level, where ν has decreased and μ has increased. Thus k will be smaller at this level than at lower levels, and absorption will be less near the tail of a burst than at earlier times. If it is assumed that absorption is negligible at the tail, then the shape of the received burst tail should be the same as that of the generated tail.

It is possible to deduce the probable shape of the generated time profile by producing the tail backwards following either an exponential curve, or a curve of the form $I^{-1/n}$ vs t (where n is 2 or 4) , to a value of t, say t_o, which corresponds to the time when the exciting source is at the f_o plasma level.

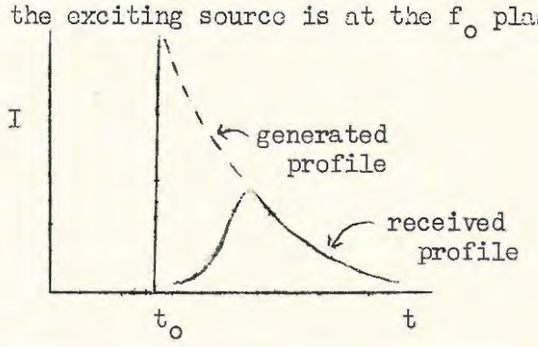

It is immaterial which law is used for this extrapolation, since all of them give approximately the same values of intensity over the range of time considered.

Comparison of the received and "generated" profiles permits an estimate to be made of the transmission loss at different parts of the burst, and the time scale can be converted to a "height in the corona" scale if the source velocity is known.

In practice, single frequency records are not suitable for use in deriving these transmission loss curves, because it is not possible either to estimate the source velocity, or to ascertain the exact position of t_o. If dynamic spectra were available it would be a simple matter to find the position of t_o for a burst observed on a frequency f_o , by taking the time at which the intensity of the harmonic band was a maximum on a frequency $2f_o$, and

also/.....

also to deduce the velocity of the exciting source.

Figure 7:9 shows a derived transmission loss curve for a typical isolated burst observed on 125 Mc./s. This was obtained by extending back the tail according to the relation $I^{-\frac{1}{2}} \propto t$ to a somewhat arbitrary value t_o situated near the start of the burst. An encouraging feature to notice is that this curve (and others obtained for other bursts in a similar manner) has more or less the shape one would expect for a transmission loss curve.

(5) Quantitative Comparison of Observations with Theory

In order to obtain useful information from the shape of instantaneous frequency profiles of isolated bursts, it is necessary to postulate that the decay of plasma oscillations at any given level is extremely rapid compared with the lifetime of a burst, so that the received shape of the band emitted from the f_o level say, is not affected by the decay of radiation arising at plasma levels lower in the solar atmosphere where $f_o' > f_o$. If the decay rate of frequencies other than f_o generated at the f_o level was known, it would be possible to calculate the effect of this decay on the shape of the instantaneous frequency profiles, but a thorough search of the literature on plasma oscillations and collision frequencies has failed to reveal any information regarding this. In any event, at high frequencies - say $f > 100$ Mc./s. - the collision frequency is probably of the order of 10 c./s., so that decay will be rapid.

Having made this point, it is now possible to decide whether the transient theory of Jaeger and Westfold (1949), in which the effect of a localized, outward moving source causing impulsive excitation at successive plasma levels is considered, gives quantitative agreement with observations. According to this theory the frequency profiles are expected to show the intensity falling off as f^{-2} or f^{-4} for frequencies appreciably greater than f_o. The author has plotted graphs of $\log_{10} I$ vs $\log_{10} f$ for the high frequency portions of isolated burst profiles from the contour diagrams of 4 typical Type III bursts recorded by

Wild/.....

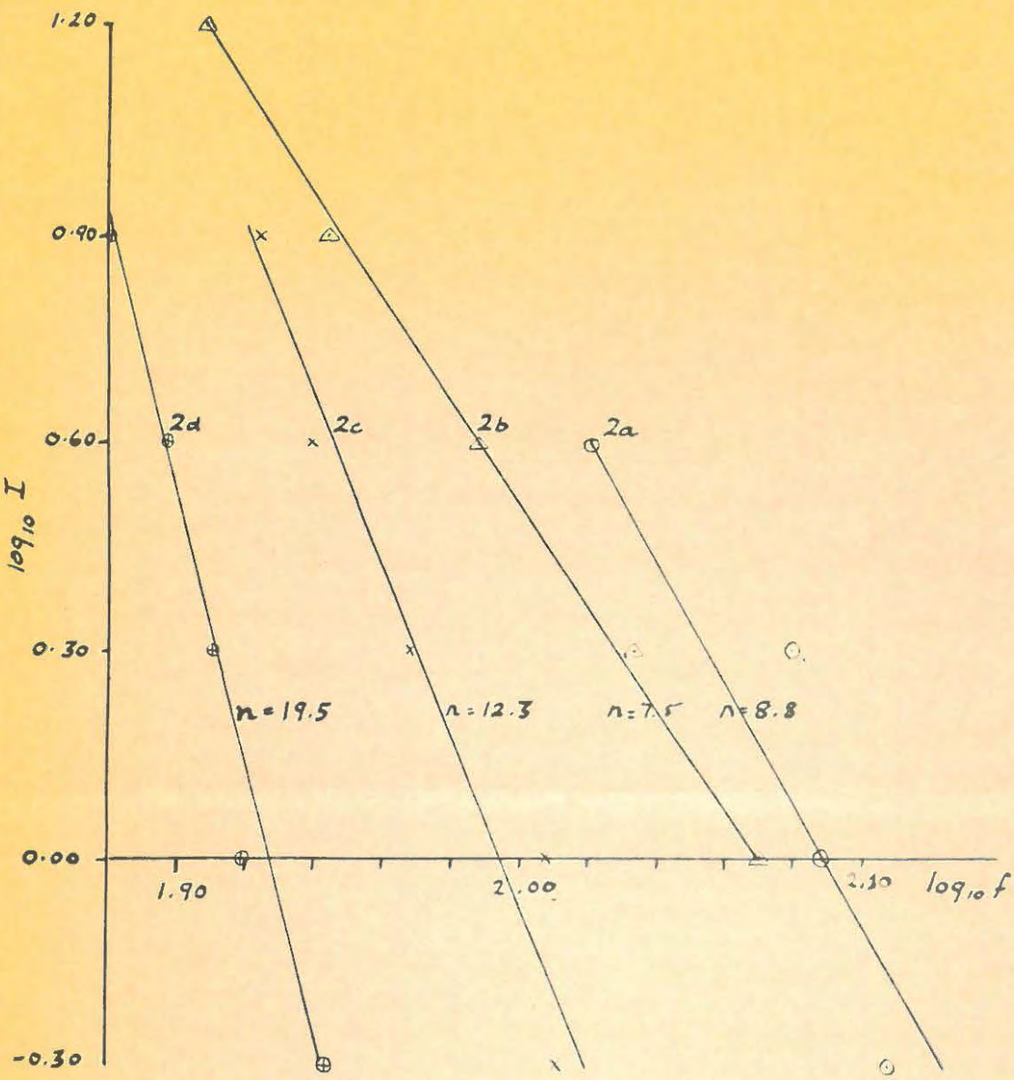

Plots of $\log_{10} I$ vs $\log_{10} f$ for the high frequency portions of instantaneous burst profiles from the contour diagrams of 4 typical Type III bursts recorded by Wild (1950b) From these graphs it appears that $I \propto f^{-n}$, and that the value of n for these bursts lies between 7.5 and 19.5.

FIGURE 7:10

Wild (1950b: Plate 2) - see figure 7:10 - and finds that $I \propto f^{-n}$ where n ranges from 7.5 to 19.5 . Inclusion of the effects of decay, the non-linear terms which were neglected by Jaeger and Westfold in deriving the spectra of transients, and the possibility that an extended source is involved may possibly account for this large discrepancy between the observed values of n and those expected on the Jaeger-Westfold theory.

E: Mechanisms Involving Wave Growth

So far in this discussion it has been tacitly assumed that excitation of radiation comprising isolated bursts is impulsive. The fact that the observed bandwidths are appreciably smaller than those expected in the transient case opens the possibility that a more coherent oscillatory process involving wave growth occurs. Two observed features of isolated bursts support this hypothesis:

(1) The peak intensity of isolated bursts is observed to increase greatly with decreasing frequency.

(2) Isolated burst sources often appear to decelerate rapidly, and become "stopped" at a fixed frequency.

A mechanism for wave growth involving a stream of particles of well defined velocity injected into a main plasma has been discussed briefly in Chapter Five. These particles, interacting with the plasma wave and giving up their kinetic energy to it, would perhaps be stopped altogether. Also, wave growth would be considerably enhanced in the direction of decreasing density, so that the intensity of emitted radiation is expected to increase greatly with decreasing frequency. If the high speed particles involved constituted a compact source, the main features of the author's model would still apply, but if an extended source was involved, interpretation of the dynamic spectra would be exceedingly difficult.

F: In Conclusion

The above hypotheses are all exploratory in nature, and more observations of isolated bursts, particularly simultaneous directional, spectral, and polarization measurements over a wide frequency range are required before any definite conclusions regarding the origin of isolated bursts can be stated. Suggestions for further research on isolated bursts, which may throw some light on the processes involved, are given in the concluding chapter.

CHAPTER EIGHT

SUGGESTIONS FOR FURTHER RESEARCH

Simultaneous polarization, directional and spectral observations of isolated bursts over a wide frequency range should reveal information of great value regarding coronal conditions existing at the time of Type III events, and of the origin, nature and movements of burst sources. A few suggested lines of approach are given below.

A: Burst Sources

Directional observations of Type III bursts over a wide range of frequencies should determine completely the paths in the solar atmosphere of burst sources. A comparison of the profiles of bursts caused by outward and inward moving sources should settle the question of whether these sources are extended or localized; a factor which is of great importance in any attempt to explain the emission of radio waves in terms of macroscopic processes. A further clue may be found by a study of the contour diagrams of isolated bursts in the region where radiation first appears.

B: Coronal Conditions

(1) Magnetic Fields

Instantaneous measurements of the complete polarization of Type III bursts throughout their lifetime may reveal information regarding the magnitude and direction of the magnetic field in the regions where emission is taking place, and also the nature of the macroscopic processes responsible for the emission.

(2) Propagation Losses

If the author's model is valid, comparison of the instantaneous frequency profiles should enable one to derive curves of the relative transmission on all frequencies above f_o arising at the f_o plasma level. From the time profiles it is possible to estimate the relative transmission of any frequency f_o arising at any

height/.....

height above the f_o level. The amount of attenuation depends mainly upon the source angle θ, and transmission curves derived in this manner over the entire range of θ for which escape of radiation is possible, would, if consistent, be of immense value in the study of bursts of solar radiation of all descriptions.

(3) Coronal Irregularities

The contour diagrams of isolated bursts recorded by Wild (1950b) show small short-lived irregularities where the radiation is either less, or more intense than the surrounding pattern. Dimensions of these irregularities are commonly in the range 0.5 - 3 Mc./s. at 100 Mc./s., corresponding to linear dimensions of 1 000 - 6 000 km. The smallest structural details observed optically in the solar atmosphere have dimensions of about 1 000 - 2 000 km., where 1 000 km. corresponds to the limit of resolution with present optical techniques. It seems reasonable to associate the irregularities in the dynamic spectra with blobs of coronal matter, thereby suggesting that a study of the extent and lifetimes of these irregularities by the radio spectrometer technique would add greatly to our present knowledge of coronal conditions.

All the above projects may be done with existing equipment, and suggest that a detailed study of isolated bursts would not only be well worth while for its own sake, but also would probably contribute greatly to the understanding of solar bursts of all types.

xxxXXXxxx

ADDENDUM

RECENT OBSERVATIONS OF ISOLATED BURSTS.

Immediately prior to publication of this thesis, two new papers dealing with isolated bursts appeared. These a re:

KOMESAROFF, M. 1958 Aust. J. Phys., 11, 201.

ROBERTS, J. A. 1958 Ibid., 11, 215.

The first deals with the polarization of Type III bursts, and Komesaroff reports that about 50% of all bursts show fairly strong circular polarization. It was previously inferred that Type III bursts were unpolarized, but this discovery is in no way contradictory to the earlier observations. Another important feature is that in polarized bursts showing a harmonic structure the fundamental band is more strongly polarized than the harmonic band. From this result Komesaroff deduces that the polarization is produced at the radiation source. In Chapter Five the author concluded that synchrotron radiation was not a possible mechanism of origin for isolated bursts, because, on the synchrotron theory, bursts are expected to show circular polarization. This conclusion is no longer valid, but the author still regards the plasma oscillation origin (which is in principle capable of giving rise to radiation exhibiting circular polarization) as being more consistent with observations, and more easily realized under coronal conditions.

The second paper reports the discovery of a new type of burst termed a "reverse drift pair" by Roberts. These bursts are not of the same class as those discussed in this thesis, but are of interest because they are also supposed to originate in a plasma oscillation process. On frequencies of about 40 Mc./s. their duration is usually less than 1 second, whereas Type III bursts have a duration of about 10 seconds. The important conclusion reached is that the lifetime of a burst on any particular frequency is not determined by the decay of oscillations of the coronal plasma after the excitation is removed, which is precisely the assumption made by the author in Chapter Seven. The rate of decay is much greater than that expected on the collision damping theory, and Twiss (unpublished) has suggested that coronal plasma oscillations would be much more rapidly damped by the diffusing effect of thermal velocities - a process known as Landau damping.

Roberts also mentions, in a footnote to this paper, that the author's interpretation of double-humped bursts is the one at present accepted by the Australian radio astronomers.

xxxXXXxxx

REFERENCES

ALFVEN, H.	1941	Arkiv för Matematik, Astronomi och Fysik, 27A, No. 25.
	1950	Cosmical Electrodynamics, (Clarendon: Oxford)
ALLEN, C. W.	1947	Mon. Not. R. Astr. Soc., 107, 426.
AZAMBUJA, M., & L. D'	1948	Ann. Obs. Paris, 6, Fasc. VII.
BAILEY, V. A.	1951	Phys. Rev., 83, 439.
BOHM, D., GROSS, E. P.	1949a	Phys. Rev., 75, 1851.
	1949b	Ibid., 75, 1864.
	1950	Ibid., 79, 992.
GILLIE, G. G., MENZEL, D. H.	1935	Harvard College Observatory Circular, 410.
DODSON, H. W., HEDEMAN, E. R., OWREN, L.	1954	Astrophys. J., 118, 169.
ELLISON, M. A.	1949	Mon. Not. R. Astr. Soc., 109, 3.
HEY, J. S., PARSONS, S. J., PHILLIPS, J. W.	1948	Mon. Not. R. Astr. Soc., 108, 354.
JAEGER, J. C., WESTFOLD, K. C.	1949	Aust. J. Sci. Res., A, 2, 322.
	1950	Ibid., 3, 376.
KRAUS, J. D.	1948	Proc. Inst. Radio Engrs., 36, 1236.
KRUSE, U. E., MARSHALL, L., PLATT, J. R.	1956	Astrophys. J., 124, 601.
LOUGHHEAD, R. E., ROBERTS, J. A., McCLURE, M. K.	1957	Aust. J. Phys., 10, 483.
MAXWELL, A., SWARUP, G.	1953	Nature, 181, 36.
MAXWELL, A., SWARUP, G., THOMPSON, A. R.	1958	Proc. Inst. Radio Engrs., 46, 142.
OWREN, L.	1954	Ph. D. Thesis, (Cornell University: New York)
PAWSEY, J. L.,	1950	Proc. Instn. Elect. Engrs., 97, 390.
PAWSEY, J. L., SMERD, S. F.	1953	Solar Radio Emission, Ch. 7 of The Sun, ed. G. KUIPER, (University of Chicago Press)
PAWSEY, J. L., BRACEWELL, R. N.	1955	Radio Astronomy, (Clarendon: Oxford)
PAYNE-SCOTT, RUBY.	1949	Aust. J. Sci. Res., A, 2, 214.
PAYNE-SCOTT, RUBY., LITTLE, A. G.	1951	Aust. J. Sci. Res., A, 4, 508.
	1952	Ibid., 5, 32.

PIDDINGTON, J. H./...

PIDDINGTON, J. H.	1955	Phil. Mag., 46, 1037.
REDMAN, R. O.	1942	Mon. Not. R. Astr. Soc., 102, 140.
RYLE, M.	1948	Proc. Roy. Soc., A, 195, 82.
	1949	Proc. Phys. Soc., A, 62, 483.
RYLE, M., VONBERG, D. D.	1948	Proc. Roy. Soc., A, 193, 98.
SCHWINGER, J.	1949	Phys. Rev., 75, 1912.
SEN, H. K.	1955	Phys. Rev., 97, 849.
SHKLOVSKY, J. S.	1946	Astr. J. (U.S.S.R.), 23, 33.
SLATER, J. C.	1942	Microwave Transmission, p. 57., (McGraw-Hill:New York and London)
SMERD, S. F.	1950	Proc. Instn. Elect. Engrs., 97, 447.
SMERD, S. F., WESTFOLD, K. C.	1949	Phil. Mag., 40, 831.
TWISS, R. Q.	1951	Phys. Rev., 84, 448.
WALDMEIER, M.	1947	Astr. Mitt. Eidgen. Sternw. Zürich, No. 155.
WESTFOLD, K. C.	1957	Phil. Mag., 2, 1287.
WILD, J. P.	1950a	Aust. J. Sci. Res., A, 3, 399.
	1950b	Ibid., 3, 541.
	1951	Ibid., 4, 36.
WILD, J. P., McCREADY, L. L.	1950	Aust. J. Sci. Res., A, 3, 387.
WILD, J. P., MURRAY, J. D., ROWE, W. C.	1954	Aust. J. Phys., 7, 439.
WILD, J. P., ROBERTS, J. A., MURRAY, J. D.	1954	Nature, 173, 532.
WILD, J.P. SHERIDAN, K. V.	1958	Proc. Inst. Radio Engrs., 46, 160.
WILLIAMS, S. E.	1948	Nature, 162, 108.